Issue No. 5 October-November 2020

LMCST
JOURNAL OF ENGINEERING & TECHNOLOGY

ISSN 2278 - 2672

Advertisement Tariff

Inside back cover (Color) : Rs. 10,000

(Black & White) : Rs. 6,000

Full page (Black & White) : Rs. 4,000

Printed and Published by

Lourdes Matha College of Science and Technology

Lourdes Hills, Kuttichal

Thiruvananthapuram-695574

Layout

Future Tech Solution

Thiruvananthapuram

foreword

Research and Development is of paramount importance in higher education. Entrepreneurship driven by innovation is the result of R&D. R&D must be focused on application based initiatives to make it useful. Though fundamental research is essential, the application of research for the development of systems is most important for overall development. Creative thinking for problem solving and analysis is essential in R&D. LMCST research advisory council is mapping out strategies for the same.

I take this opportunity to congratulate the authors and the members of the editorial board for their dedicated efforts to contribute for quality research papers useful for the scientific community. I have immense appreciation for the entire team who made this edition of the journal a reality

Rev. Fr. Dr. Tomy Joseph Padinjareveettil

Director

foreword

Research and Development is the primary objective of higher education. Innovation and Entrepreneurship are the offshoots of R&D. When R&D is focused on societal needs, it becomes useful for the growth of the country as a whole. Though pure research is essential fundamentally, the application of research for the development of useful products and systems is the most important for societal development. This needs continuous updating of learning, critical thinking for problem solving and analysis. To cater to these needs, LMCST research advisory council is working out strategies in a systematic manner including quality research journal publication.

I take this opportunity to congratulate the authors and the members of the editorial board for their dedicated efforts to contribute for quality research papers useful for the scientific community. I have immense gratitude for the entire team who made this edition of the journal published meeting all the requirements.

Dr. Mohanlal P. P.

Principal

CONTENTS

Solar Energy Scenario in India

M.V. Bindu

Associate Professor, Dept. of Mechanical Engineering, LMCST, PhD scholar, NICHE, Noorul Islam Centre For Higher Education, Kumaracoil, Thuckalay,K.K.Dist,Pin-629 180
Thuckalay,K.K.Dist,Pin-629 180
bindumvmohanan@gmail.com.

***Abstract*— India with a population of 133.92 crores largely depends on the conventional source of energy for meeting the energy demand. The dependency on the fossile fuel leads to the greenhouse gas emissions which adversely affect the society and the environment. The need for the hour is the sustainable energy and this drives us to focus on the solar energy sources. India is located in the tropical region which receives the 4e7 kW h per square metre per day (kWh/m2/day) and therefore the solar resource become an alternative energy sources. In this paper the current scenario of solar energy utilisation in different sectors and the policies for the growth in this area is reviewed and presented.**

***Keywords*—Solar irradiation, PV modules**

INTRODUCTION

India is the second-largest populated country in the world, with an area of 3.287 million km² and geographic coordinates located at latitude 20.5936832, longitude 78.962883. With a population of 133.92 crores, the energy demand is increasing rapidly which is met by the fossil-based power plants. The dependency on these power plants will increase the greenhouse gas emissions, adversely affecting the society and environment. The slow development of the power sector in India has left rural households with poor quality and unreliable power supply. Even though the grid extension is the traditional approach to meet the rising energy demand, to fulfill the continuously growing appetite for the power supply, India needs to find an alternative sustainable source of energy. Among many available options of renewable energy, solar photovoltaic is the best alternative for distributed energy generation.

The Solar energy is an alternate solution to overcome the current situation and the Government of India has set a target of installing 40 GW of decentralized solar rooftop PV up-to 2022(Wiki). In this paper the solar irradiation availability in different part of the country, solar energy production in different sectors and the solar power policies adopted for the decentralized solar rooftop PV segment is highlighted.

SOLAR IRRADIATION AVAILABILITY IN INDIA

India is having 250 to 300 sunny days and a solar radiation potential of 5000 trillion kilowatt hour per year (kWh/year), which is more than sufficient to generate electricity from solar photo-voltaic (PV) and solar thermal power applications, for an year [1]. According to the National Renewable Energy Laboratory, the annual average direct normal irradiance in most of the states of India is around 4.5 to 5.0 KWh/m2/Day and average global horizontal irradiance is around 5.0 to 5.5 KWh/m2/Day. This solar

energy is sufficient to produce 6,081,709 TWh/year in the world. A solar radiation atlas of India developed by MNRE in collaboration with German consulting company Suntrace GmbH is shown in Fig. 2. The Global Horizontal Irradiance (GHI) shows that most the Indian subcontinent receives more than 5 KWh/m2/day. It has been estimated that around 1.89 million km2 of the geographical area receive annual mean GHI of 5 KWh/m2/day [Wiki]. The GHI available in different part of the country is given in the Table.1.

Table.1.GHI In India

Places, India	GHI
New Delhi	5.069 KWh/m2/day
Rajasthan	5.5e6.8 kWh/m2/day
Jhodpur	5.54 KWh/m2/day
Ahemdabad	5.36 KWh/m2/day
Mumbai	5.069 KWh/m2/day
Pune	5.41 KWh/m2/day
Hyderabad	5.65 KWh/m2/day
Chennai	5.069 KWh/m2/day
Banglore	5.47KWh/m2/day
Thiruvananthpuram	5.40 KWh/m2/day

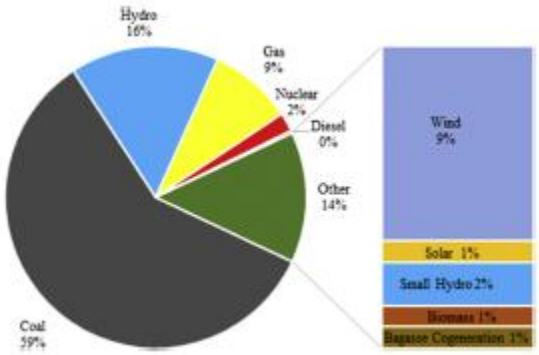

Fig.1.Energy usage from all technology [ref2]

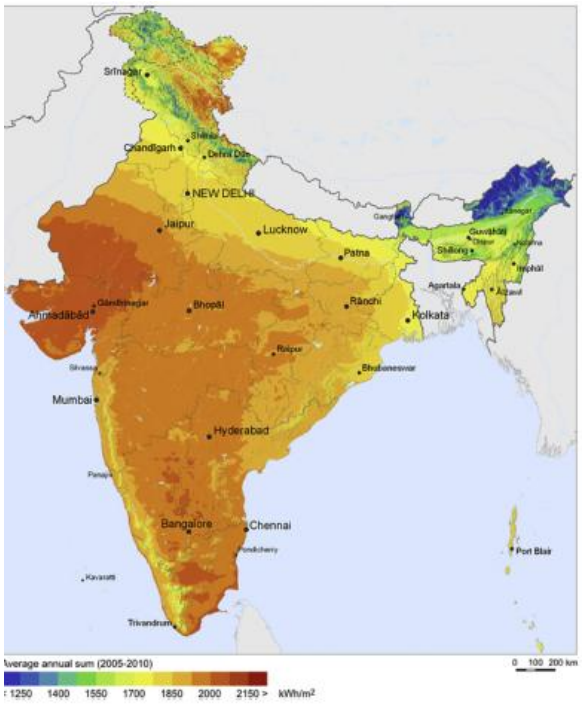

Fig.2.Solar irradiation availability in states of India

The current energy usage energy from the fossile and different energy production technology in India is shown in the Fig. 1.

SOLAR ENERGY POLICIES AND PRODUCTION

A. Jawaharlal Nehru National Solar Mission (JNNSM)

The Jawaharlal Nehru National Solar Mission (JNNSM) under the National Action Plan on Climate Change (NAPCC) was launched in 2010-2011 by the Government of India with the target to deploy 20,000MW of grid connected power, 2,000MW off-grid solar applications of 20 million solar lights, 20 million sq.m. solar thermal collector area, and to develop the manufacturing capacity and for the R & D work by the year 2022.{14}. The implementation of the program will be through various

agencies such as Solar Energy Corporation of India (SECI), State Nodal Agencies (SNA), Channel partners, and Financial Institutions etc.

B. National Action Plan on Climate Change (NAPCC)

Post- National Action Plan on Climate Change (NAPCC), 2008 The NAPCC for solar energy development in India through the Renewable Purchase Obligation (RPO) and Renewable Energy Certificates (REC) trading mechanism. The RPO framework formulated under the EA 2003 mandates individual states to procure at least 5% of power from RE sources by 2010 and subsequently increase by 1 percentage-on-year for the next 10 years.

C. Solar Energy Capacity

The solar installed capacity in India reached 33.730 GW as of 31 December. The capacity is targeted to be 100 GW including 40 GW from rooftop solar by 2022. Dharnai in Bihar is the first Indian village which is powered entirely by solar electricity. The Indian city of Agra, is to become the country's first solar city. The energy production in India is given in the Table.2

Table.2.Installed Energy Capacity

Installed cumulative National and State wise Capacity		
Stae	31 March 2015	31 March 2017
Gujarath	1,000.05	1,249.37
Maharastra	360.75	452.37
Chattesgarh	7.60	128.86
Madhya Pradesh	558.58	857.04

SOLAR ROOFTOP IN INDIA

Solar rooftop PV is an emerging technology and is a sustainable option among the decentralized power generating systems like Diesel Generator and family sized biogas power system. In India, the cumulative solar PV installation is more than 9012 [2]. Out of this total installed capacity, around 80% of the solar rooftop PV systems were installed under CAPEX model and only 20% were installed under RESCO model as shown in Fig. 3.

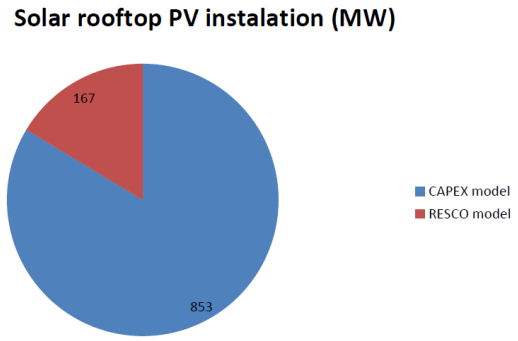

Fig.3. Solar Roof Top in India

In the past 2 years, the annual growth of the rooftop solar photovoltaic segment was about 90%. Around 73% of the rooftop market is captured by Commercial and Industrial (C&I) segment and remaining 27% is covered by the residential segment [2]. Fig. 4 shows the state wise distribution of solar PV installed capacity up to September 2016. The cumulative installed capacity of solar rooftop segment in India is 1020 MW as of September 2016.

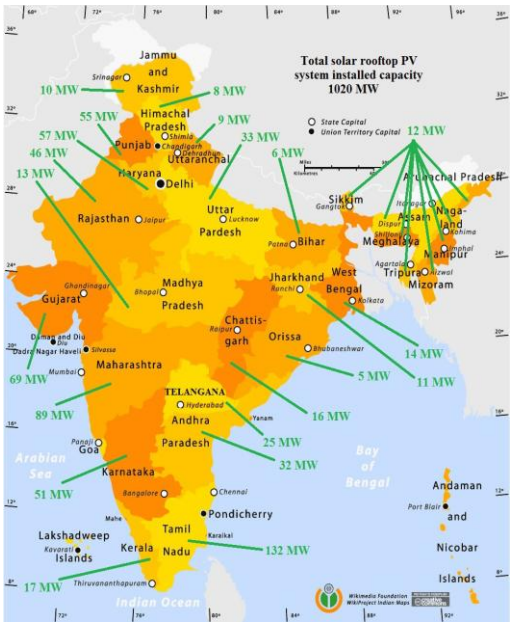

Fig.4.Solar rooftop PV in India

SOLAR WATER PUMPING

In India, fossil fuel-based water pumps are used for irrigation. The solar energy which is available in abundance can be used for the irrigation purpose using the Solar Photovoltaic Water Pumping (SPVWP) technology.

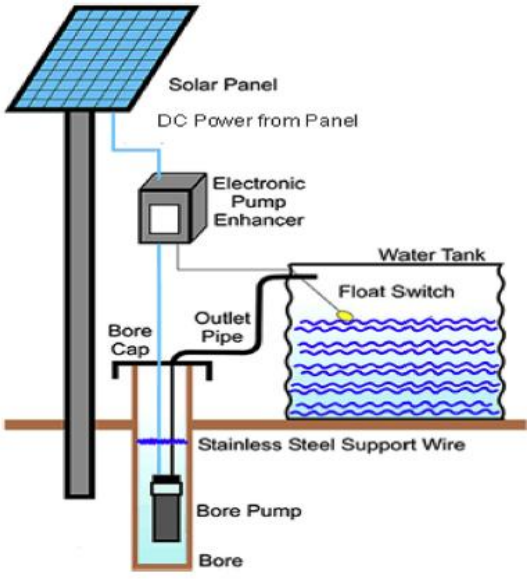

Fig.5.SPVWP

For irrigation and drinking water the SPVWP system is promoted through Ministry of Renewable Energy Resources (MNRE). A PV module 900 Watt to 9KWp of capacity is needed for the SPVWP system In India only 38,964 SPVWP units were installed since 1993. The schematic of the SPVWP is shown in the Figure.5.

COCHIN INTERNATIONAL AIRPORT LIMITED (CIAL)- CASE STUDY

On an average, the daily electrical energy requirement of Cochin Airport is around 50,000 units (Cochin International Airport Limited (2016). The electrical requirement includes the airside energy demand and landside energy demand.

The 1.1 MW solar plant was commissioned in 2013 in an area of 45 acres (184,668 m2). The solar plant is located at 10.157 N, 79.383 E at an altitude of 6 m. The site receives ample amount of global horizontal irradiation throughout the year (1930.9 kWh/ m2/year) (NASA SSE). This PV plant consists of 46150 polycrystalline PV modules of 260Wp rating. The operating parameter of PV module is given in Table 2. The number of module was increased by adding 9240 polycrystalline PV modules to the existing one in 2016. The modules are oriented south at angle of 10_ from the horizontal.

The specifications of 14.4 MWp solar PV plant is given in Table.3. The module specification is in Table.4 and the inverter specification is in Table.5.

Table.3. Specifications of 14.4 MWp solar PV plant

Parameter	Description	Modified with
Site Coordinates	10.157_N, 76.383_E	
Type of Solar Module	Poly e Si 260 Wp	Poly e Si 260 Wp
Number of PV modules	46150	9240
Tilt angle	10_ (fixed tilt)	10_ (fixed tilt)
No of modules per string	25	24
No of strings	1846	385
No of inverters	10 nos of 1 MW	2 nos of 1 MW
No of transformers	5 nos of 2 MV A	1 nos of 2 MV A

Table.4.PV Module Specifications

Parameter	Value
Manufacturer	ReneSola
Conversion Efficiency	15.8%e16.2%
Short circuit current	(ISC) 8.95 A
Open circuit voltage	(VOC) 37.6 V
Operating Temperature	40 _Ceþ85 _C
Dimension	1640 _ 990 _ 40 mm (19 kg)

.

Table.5.Inverter Specifications.

Design Parameter	Value
Power output	1 MW
Efficiency	98.8%
DC input	600 Ve850 V
AC output	400 V & 1445 A
Total Harmonic Distortion (THD)	3%_

CIAL Solar Power Project is a 15 megawatt (MW) photovoltaic power station built by CIAL. Cochin International Airport became the first fully solar-powered airport in the world with the commissioning of the plant.

PV modules can be installed on roof top, over car parking area, utilised land area and can also be integrated with building. Cochin International Airport Limited (CIAL) came into operation commissioning in 2013. 80 String Combine Boxes (SCB) installed with 25 PV modules connected in series to form a string. . In the string in 2016 have 24 PV module connected in series. The DC lines from eight SCB's are fed into an inverter. The inverter or power conditioning unit has an inbuilt maximum power tracking facility. Twelve inverters of 1 MW are used and are placed in three separate power block stations. There are six transformers of 2MV A rating in the PV power plant and are used to step up the low voltage AC output from the inverter.

Each transformer is connected to inverters and the power generated is transferred to 11 kV\110 kV substation situated near to project site.

Fig.6. 14.4 MWp Solar Power Plant

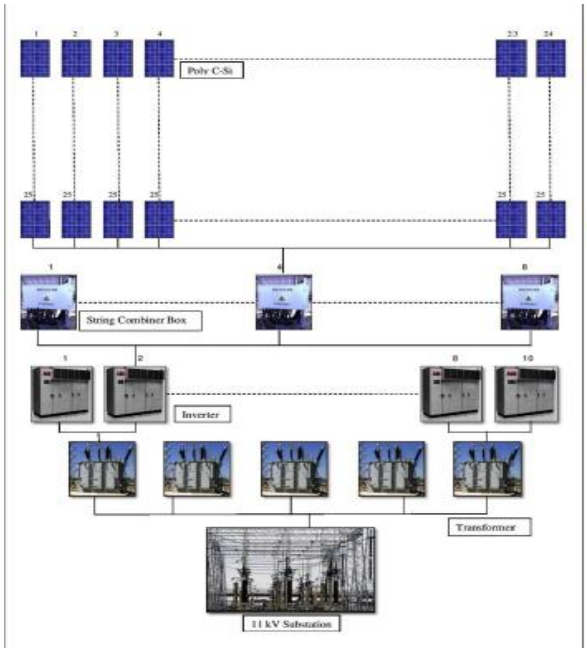

Fig.7: Schematic diagram of 14.4 MWp grid connected PV Plant

CONCLUSION

The solar sector in India has broader possibilities which can be realised with the help of different Government Policies. India has large area receiving the solar irradiation which can be utilised for developing solar power plants. The 1.1 MW PV solar power plants in Gujarat developed over the Narmada canal make the land engagement, as well as helps in saving 7 million liters of drinkable water annually. The 14.4 MWp solar PV plant in the Cochin International Airport is meeting the electrical energy requirement of the airport. The development of India, economically, socially and environmentally is possible by tapping the solar energy sources.

References

Komali Yenneti The grid-connected solar energy in India: Structures and challenges Energy Strategy Reviews Energy Strategy Reviews 11-12 (2016) 41e51

Pushpendra Kumar Singh Rathore, Durg Singh Chauhan, Rudra Pratap Singh, Decentralized solar rooftop photovoltaic in India: On the path of sustainable energy security,Renewable Energy (2018), doi: 10.1016/j.renene.2018.07.049

Pushpendra Kumar Singh Rathorea,b,, Shyam Sunder Dasb, Durg Singh Chauhan Perspectives of solar photovoltaic water pumping for irrigation in India Energy Strategy Reviews Energy Strategy Reviews 22 (2018) 385–395

Fully solar powered airport: A case study of Cochin International airport, Journal of Air Transport Management Journal of Air Transport Management 62 (2017) 176e188

AUTHOR

Ms. Bindu M V, Associate Professor, Department of Mechanical Engineering, B.Tech and M.Tech form College of Engineering

Trivandrum, Kerala, currently perusing Ph.D in Noorul Islam Centre for Higher Education, Department of Mechanical Engineering in the research area Renewable Energy (Solar Energy) Sources. 16 Years of experience in the teaching profession and one year in Industry. Joined LMCST in 2006 August. Participated and presented two papers in two international conferences and gh published the papers in journals. Total number of publications-5.

Classification of Local Patches extracted from Magnetic Resonance Images using Machine Learning to identify Iron depositions in brain

Beshiba Wilson

Associate Professor and HOD,Department of Computer Science and Engineering, Lourdes Matha College of Science and Technology

beshiba.wilson@lmcst.ac.in

***Abstract* — Neurodegenerative diseases are a group of disorders that are characterized by the progressive brain disorder that causes uncontrolled movements, emotional problems, and loss of thinking ability (cognition). It leads to progressive degeneration of the structure and function of the central nervous system which leads to Alzheimer's disease, Huntington disease and Parkinson's disease. Iron deposition in brain has been observed with normal aging and is associated with neurodegenerative diseases. The classification of brain Magnetic Resonance (MR) images based on iron deposition in Basal Ganglia region of brain is very difficult to using simple MRI techniques. The MRI sequence namely Susceptibility Weighted Imaging (SWI) helps to distinguish brain iron regions. The objective of this research work is to investigate the iron regions in Basal Ganglia region of brain and classify MR images. This study included 15 MRI subjects with iron region and 15 healthy controls. A total of 120 localized patches were constructed based on iron and normal regions. Gray Level Co-occurrence Matrix (GLCM) features are extracted from the patches and fed to Support Vector Machine (SVM) Classifier The SVM Classifier was used to train and test the performance accuracy in the detection of iron region in brain MRI Images. for patch based classification of iron region. The experimental results shows that the proposed localized patch based approach for classification of brain iron images using the efficient machine learning technique namely, Support Vector Machine achieved 95.7% classification accuracy in identifying normal and iron regions from brain MR images.**

***Keywords*— Neurodegenerative diseases, Susceptibility Weighted Imaging, Basal Ganglia, Gray Level Co-occurrence Matrix, Machine Learning.**

I. INTRODUCTION

One of the main causes for human cognitive aging is deposition of iron in the form of hemosiderin in many regions of brain [1]. Neurodegeneration with accumulation of brain iron leads to neurodegenerative diseases [2]. Increased quantity of iron in brain has been related to chronic brain disorders like Alzheimer's disease, movement disorders particularly Parkinson's disease and dystonia, multiple sclerosis, cognitive dysfunction, retinal abnormalities and other disorders [3]. Seven Neurodegeneration with brain iron accumulation (NBIA) disorders are related with emphasis on neuroimaging and clinical syndromes [4]. It is evident that there is age-related deposition of iron in five regions of brain (Substantia Niagra, Putamen, Red

Nucleus, Dendate Nucleus and Caudate) from T2-weighted MRI spin-echo image [5]. MRI (Magnetic Resonance Imaging) studies shows that in most forms of NBIA, the iron deposition mainly occurs in the crucial brain regions of Basal Ganglia[2] such as Globus Pallidus [6], Putamen and Caudate [7]. Reference [8] shows that Globus Pallidus, Putamen and Caudate are categorized under Basal Ganglia and related nuclei. Sample MRI sequences of T1 and T2-Weighted images are shown in Figure 1.

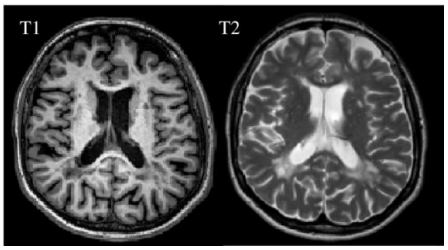

Fig. 1: Sample MRI sequences T1 and T2-Weighted images

A neuroimaging technique in which the magnetic susceptibility differences of tissues is used to enhance contrast of MRI is known as Susceptibility Weighted Imaging (SWI) [9]. A sample image sequence of SWI is shown in Figure 2.

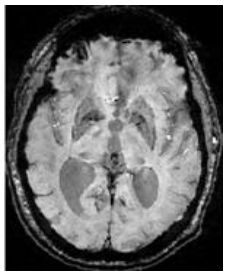

Fig. 2: Sample image sequence of Susceptibility Weighted images

Reference [10] suggests that a quantitative assessment of iron deposition with SWI reveals a new biomarker for frontotemporal dementia. The detection of iron content in brain facilitates efforts to provide treatments for the associated neurodegenerative disorders.

In this research work, a novel technique for extraction of brain features based on localized patch features is implemented. One of the efficient machine learning techniques namely Support Vector Machine is used to classify the iron regions in brain. The rest of this paper is organized as follows: Section II describes related works. Section III gives the details of dataset used in this research work. Section IV illustrates the proposed work. Section V presents the results and discussion. Section VI discusses about conclusion.

II. RELATED WORKS

The quantification of iron in MRI brain images is a significant area of research nowadays. Though identification of iron content in brain using automated techniques is not fully developed, similar work has been carried out in the automated identification of tumor region in brain. A survey on the stages involved in the automated identification of tumor region in brain namely feature extraction, segmentation and classification are discussed. Features are the important characteristics of an image and texture is the most important feature of an image. Reference [11] suggests that the statistical method of examining the textures is Gray Level Co-occurrence Matrix (GLCM) and it considers spatial relationship between the pixels.

Reference [12] shows the Enhanced Darwanian Particle Swarm Optimization (EDPSO) method which is used for identification and segmentation of tumor in MRI. Reference [13] explains four clustering techniques namely Mean Shift, Fuzzy C-means, K-means and Maximization Expectation for detecting mass tumor in brain.

Reference [14] introduces a Support Vector Machine (SVM) based Recursive Feature Elimination (RFE) is used to determine a subset of features based on backward sequential selection method and optimizes the performance of the classifier. Reference [15] describes an automated classification method based on Eigen brains and SVM machine learning technique to detect Alzheimer's disease related brain regions in 3D MR images. Reference [16] illustrates a study on recent segmentation and tumor classification methods of brain MRI. The current trends in segmentation and classification related to tumor are elucidated. Reference [17] describes Probabilistic Neural Network (PNN) to train and test the performance accuracy in identification of tumor region in brain MR images.

III. DATASET

The Oasis-3 dataset [18] is used in this research work. The slices includes axial view of Susceptibility Weighted Images (SWI) of 3.0 Tesla MR Sessions obtained using Siemens TIM Trio 3T MRI Scanner. The brain image subjects includes 15 cases both men and women aged 60 to 80 with iron regions and 15 healthy controls. The iron regions in each image were outlined with the help of experienced radiologist. Such marked images are used as ground truth images. The scientific computing using Python – Version 3.6.7 and Scikit -image Package as software tools is used for implementation purpose.

IV. PROPOSED WORK

The proposed work for classification of iron regions in brain comprises of the fundamental stages such as Region of Interest (ROI) Selection, Construction of local patches, Feature Extraction and Classification. Figure 3 illustrates the steps of our proposed work. We propose a novel patch-based approach using robust classification techniques to identify and classify iron regions in brain MRI.

The regions of interest of brain MRI includes three main parts of Basal Ganglia namely Globus Pallidus, Putamen and Caudate. The SWI image slices showing these regions are selected for image manipulations. All the original images are available in RGB format. Initially, the RGB images are converted into gray scale images.

SWI Images are usually prone to Gaussian and Rician noise. The Gaussian smoothing is performed on the gray scale image by applying Gaussian function which filters the noise in the image. The iron content in the regions under consideration are analyzed with the help of an expert radiologist and the images are considered to be the ground truth.

The influence of patch size on accuracy of the classification is a significant research area under consideration. The main regions of basal ganglia namely caudate, putamen and globus pallidus are used in this research. After selection of ROI, core pixels of iron and normal regions are identified. Based on the core pixels as center, patches in iron and normal regions are generated. Table 1 shows that the influence of various patch sizes including 5 x 5, 10 x 10, 15 x 15 and 21 x 21 on the accuracy of the system.

The patches generated are stored in the template patch library. The size of patch is an important factor in determining the accuracy of the entire iron identification system. The efficiency of the system is comparatively more for the patch size of 21 x 21. Greater values of patch size than 21 x 21 will be inefficient since the iron detection is done on a pixel by pixel basis. Thus the patch size is fixed to be 21 x 21

for iron and normal regions.

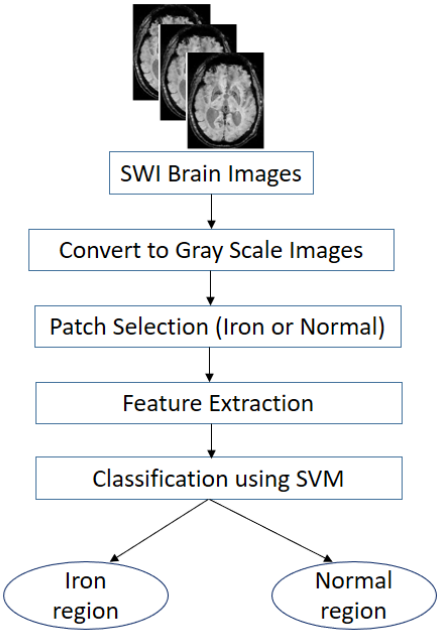

Fig. 3: Flowchart of proposed work

Table 1: Influence of Patch Sizes 5 x 5, 10 X 10, 15 X 15 and 21 X 21 on the Accuracy of the Proposed Work

Patch Size	Accuracy (%) of the Proposed Work
5 x 5	88.7
10 x 10	91.45
15 x 15	93.76
21 x 21	94.32

Table 2 shows the sample values of patch based GLCM Features namely dissimilarity, correlation and contrast extracted from three specific cases of iron and normal regions.

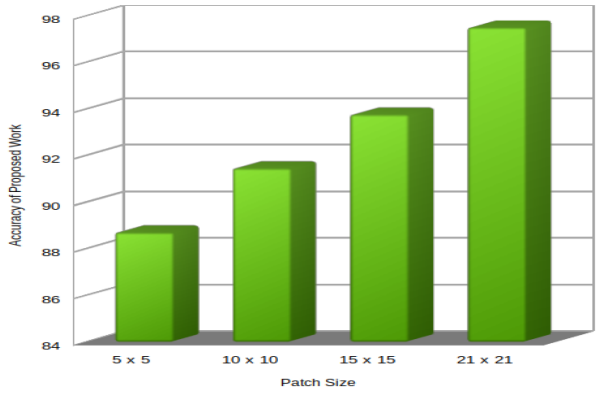

Fig. 4: Graphical Representation of the Influence of Patch Sizes 5x5, 10 X 10, 15 X15 And 21 X 21 on the Accuracy of the Proposed Work

Table 2: Patch Based GLCM Features - Dissimilarity, Correlation and Contrast Extracted From Three Cases of Iron and Normal Regions in Brain MRI.

Case/Features	Dissimilarity	Correlation	Contrast
Iron region 1	32.08	-0.0299	1218.95
Iron region 2	31.38	-0.0516	1656.57
Iron region 3	34.93	-0.019	1358.33
Normal	20.24	0.12	632.41

region 1			
Normal region 2	23.08	0.126	702.23
Normal region 3	22.85	0.127	755.3

Though all the fourteen Haralick's features were extracted, only the sample values of GLCM features are provided for some specific regions of iron and normal cases. It is seen from the results that there is a wide variation in the values of dissimilarity, correlation and contrast between the iron and normal regions. This paves the way for a detailed research being carried out on the features extracted during the feature extraction process.

Table 3 shows sample values of patch based GLCM features such as homogeneity, ASM and energy extracted from specific cases of iron and normal regions. It also shows that there is a wide variation in the values of as homogeneity, ASM and energy between the iron and the normal regions.

Table 3: Patch Based GLCM Features - Homogeneity, ASM and Energy Extracted From Three Cases of Iron and Normal Regions in Brain MRI.

Case/ Features	**Homogeneity**	**ASM**	**Energy**
Iron	0.0908	0.0073	0.0934
region 1		3	
Iron region 2	0.0862	0.00756	0.0935
Iron region 3	0.103	0.00737	0.0954
Normal region 1	0.0398	0.00628	0.0793
Normal region 2	0.0409	0.0064	0.0682
Normal region 3	0.0388	0.00558	0.0747

During the process of feature extraction, fourteen features are extracted from twenty patches each of iron and normal regions. Figure 5 shows the representation of features extracted using dissimilarity and correlation GLCM methods in iron and normal regions.

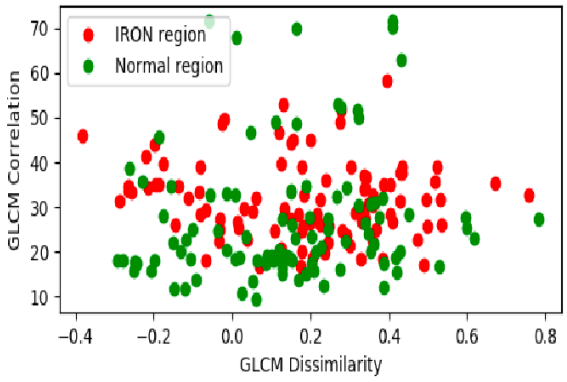

Fig. 5: Representation of Features Generated Using Correlation and Dissimilarity Methods.

A total of 560 features are extracted for an image. In this proposed system, we extract both

gray scale and gradient features from the images. The gradient features are extracted using Sobel, Prewitt and Robert's gradient operators. A total of 560 features each is required for the gradient operators.

This increases the number of features extracted for a particular image. For efficient processing, the number of images must be reduced.

After the process of extraction of the features, the feature scaling is performed. Since the GLCM features are having varying diversity SVM produces better results compared to the LR method. When the feature scaling is performed on training data, the proposed method using Random Forest Classifier gives optimal results.

After reduction of features using PCA, the values of the weighted coefficients of gray scale (αg) and gradient scale coefficients namely Sobel (αs), Prewitt (αp) and Roberts (αr) are determined. These weighted coefficients are assumed to be a constant number which adds weightage to the discriminative feature. Using grid search technique, it is found that the gradient scale coefficient of Prewitt influences the weighted coefficient to a greater extent. Thus the discriminative features are computed based on the two weighted coefficients namely gray scale and Prewitt gradient scale coefficients. To increase the accuracy of the classifier, optimal values are determined for the weighted coefficients are determined using grid search technique. Table 4 shows the optimal values for αg and αp using grid search based on classifier accuracy. Figure 8.9 shows the graphical representation of the optimal values for αg and αp using grid search based on classifier accuracy.

Table 4: Determination of Optimal Values for αg and αp using grid search Based on Classifier Accuracy.

Classifier Accuracy	**αg =0.3 & αp=0.7**	**αg =0.4 & αp=0.6**	**αg =0.3 & αp=0.8**
LR	71.25	75	68.75
Linear SVM	83.75	86.67	87.5
Kernel SVM	93.25	97.5	92.75

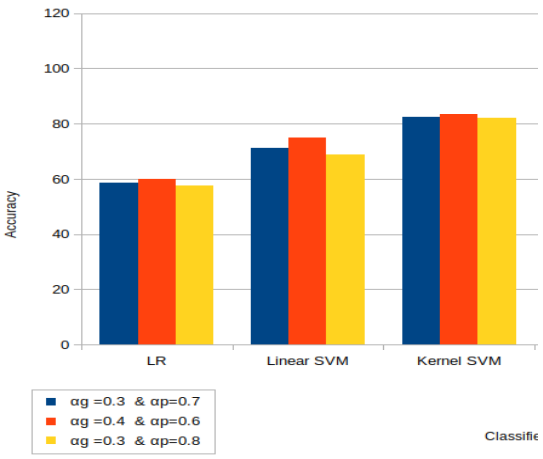

Fig. 6: Graphical Representation of Optimal Values αg and αp and Variations in Accuracy of Classifiers

After determination of the discriminative features, the classification of the images is performed by various classifiers like LR, linear SVM and kernel SVM. The Kernel SVM

Classifier

classifier shows better performance compared to other traditional methods.

The variations of estimators with classification accuracy is illustrated in graphical form. A comparative analysis using three state of the art and most widely used machine learning classifiers is performed. The classifier accuracy of various classifiers are presented in Table 5.

Table 5: Classification Accuracy Scores of Various ML Algorithms

Sl. No.	Classifier	Classification Accuracy (%)
1	Logistic Regression	75
2	Linear SVM	63
3	Kernel SVM (RBF)	95.7

Figure 7 shows the graphical representation of the classifier accuracy of various classifiers.

The accuracy of the proposed method is calculated based on the number of correctly classified images and wrongly classified images. From the analysis conducted it is clear that the hybrid technique extraction of discriminative features using innovative method followed by SVM classification yields the highest accuracy of 97.5

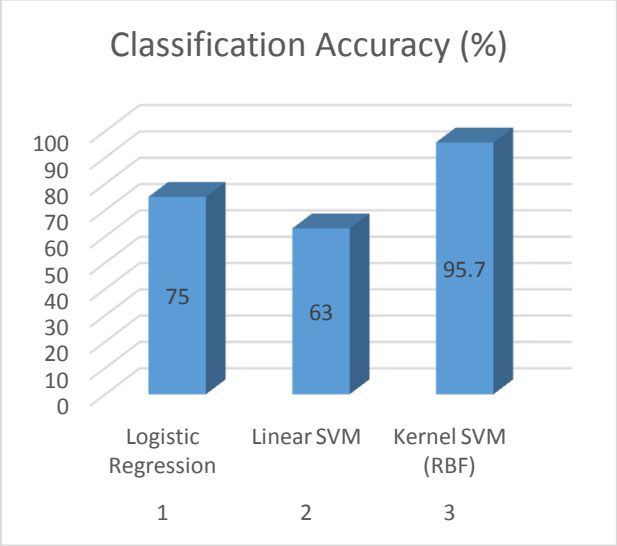

Fig. 7: Comparative Analysis of Classifiers Based on Accuracy

V DISCUSSION

To validate the performance of this research work, 120 MR images (slices of SWI Axial view) of brain with iron content were taken from Oasis Brains Datasets. The ground truth images were generated by selection of ROI manually with the help of an expert radiologist. Totally 560 features were obtained from the 20 iron patches and 20 normal patches for each image based on the fourteen Haralick's features.

VI CONCLUSION

The detection of iron region in Neurodegeneration with Brain Iron Accumulation is important for the diagnosis and treatment of iron overload in various neurodegenerative diseases. This paper presented

a novel feature extraction approach for identification and classification of iron region in brain. The local patch based approach is combined with the feature extraction techniques to determine the powerful features from the given image. The patch based features gives 95.7% classification accuracy with robust classifier like Kernel SVM Classifier. The experimental results shows that the classification accuracy obtained by using the proposed novel features is high compared to other state of art classification techniques.

ACKNOWLEDGMENTS

Data were provided by OASIS- 3 dataset. Principal Investigators: T. Benzinger, D. Marcus, J. Morris; NIH P50AG00561, P30NS09857781, P01AG026276, P01AG003991, R01AG043434, UL1TR000448, R01EB009352. AV-45 doses were provided by Avid Radiopharmaceuticals, a wholly owned subsidiary of Eli Lilly.

REFERENCES

[1] Maria del C. Valdes Hernandez, Stuart Ritchie, Andreas Glatz, Mike Allerhand, Susana Munoz Maniega, Alan J. Gow, Natalie A. Royle, Mark E. Bastin, John M. Starr, Ian J. Deary and Joanna M. Wardlaw , '*Brain iron deposits and lifespan cognitive ability*', AGE (Springer),2015, 37:100.

[2] M.C. Kruer, N. Boddaert, S.A. Schneider, H. Houlden, K.P. Bhatia, A. Gregory, J.C. Anderson, W.D. Rooney, P. Hogarth and S.J. Hayflick, '*Neuroimaging Features of Neurodegeneration with Brain Iron Accumulation'*, AJNR Am J Neuroradiol, 2012, 33:407–14.

[3] Rubens Paulo Araujo Salomao, Jose Luiz Pedroso, Maria Thereza Drumond Gama, Livia Almeida Dutra, Ricardo Horta Maciel, Clecio Godeiro-Junior, Hsin Fen Chien, Helio A. G. Teive, Francisco Cardoso and Orlando G. P. Barsottini, ' *A diagnostic approach for neurodegeneration with brain iron accumulation: clinical features, genetics and brain imaging'*, Arq Neuropsiquiatr, 2016, 74(7):587-596.

[4] Hyman M. Schipper, '*Neurodegeneration with brain iron accumulation — Clinical syndromes and neuroimaging'*, Biochimica et Biophysica Acta 1822, 2012, 350–360.

[5] Laura 0. Thomas, Orest B. Boyko, Douglas C. Anthony and Peter C. Burger, *'MR Detection of Brain Iron'*, AJNR, 1993, 14 :1043- 1048.

[6] Michael C. Kruer, '*The Neuropathology of Neurodegeneration with Brain Iron Accumulation'*, Int. Rev. Neurobiol., 2013, 110: 165–194.

[7] Shen-Qiang Yan, Jian-Zhong Sun, Yu-Qing Yan, He Wang and Min Lou, *'Evaluation of Brain Iron Content Based on Magnetic Resonance Imaging (MRI): Comparison among Phase Value, R2* and Magnitude Signal Intensity'*, PLoS ONE Vol.7, Issue 2, 2012.

[8] Jose L. Lanciego, Natasha Luquin and Jose A. Obeso, *'Functional Neuroanatomy of the Basal Ganglia'*, Cold Spring Harb. Perspect. Med, 2012.

[9] E.M. Haacke, S. Mittal, Z. Wu, J. Neelavalli and Y.-C.N. Cheng, *'SusceptibilityWeighted Imaging: Technical Aspects and Clinical Applications, Part 1'*,AJNR Am J Neuroradiol, 2009, 30:19 –30.

[10] R. Sheelakumari, C. Kesavadas, T. Varghese, R.M. Sreedharan, B. Thomas, J. Verghese and P.S. Mathuranath, '*Assessment of Iron Deposition in the Brain in Frontotemporal Dementia and Its Correlation with Behavioral Traits'*, AJNR Am J Neuroradiol, 2017.

[11] Priyanka Udayabhanu , Anjaly Viswan and Seema Padmarajan, '*MRI Brain Image Classification using GLCM Feature Extraction and Probabilistic Neural Networks'*, International Conference on Emerging Trends in Engineering & Management (ICETEM), 2016.

[12] Vasupradha Vijay, A.R.Kavitha and S.Roselene Rebecca, *Procedia Computer Science* 92 – Elsevier, 2016, 475 – 480.

[13] Eman Abdel-Maksoud, Mohammed Elmogy and Rashid Al-Awadi Brain, '*Tumor segmentation based on a hybrid clustering technique'*, Egyptian Informatics Journal 16, 2015, 71–81.

[14] Evangelia I. Zacharakia, Sumei Wanga, Sanjeev Chawlaa, Dong Soo Yooa, Ronald Wolfa, Elias R. Melhema and Christos Davatzikosa, '*Classification of brain tumor type and grade using MRI texture and shape in a machine learning scheme'*, Magn Reson Med., 62(6), 2009, 1609–1618.

[15] Yudong Zhang, Zhengchao Dong, Preetha Phillips, Shuihua Wang, Genlin Ji, Jiquan Yang and Ti-FeiYuan, '*Detection of subjects and brain regions related to Alzheimer's disease using 3D MRI scans based on eigen brain and machine learning'*, Frontiers in Computational Neuroscience, Vol.9, Article 66, 2015.

[16] Geethu Mohan and M. Monica Subashini, '*MRI based medical image analysis: Survey on brain tumor grade classification'*, Biomedical Signal Processing and Control, 39, 2018, 139–161.

[17] N. Varuna Shree and T. N. R. Kumar, '*Identification and classification of brain tumor MRI images with feature extraction using DWT and probabilistic neural network'*, Brain Informatics,Vol.5, 2018, 23–30.

[18] Oasis Brains Datasets - http://www.oasisbrains.org.

Prof. Beshiba Wilson started her career in teaching since 2003 and is presently the Head of

the Department of Computer Science and Engineering in Lourdes Matha College of Science and Technology. She is an M.Tech graduate in Computer Science and Engineering. Currently she is pursuing research in the field of Machine Learning and Medical Imaging. She has taught a variety of computer courses including Neural Networks, Computer Graphics, Python Programming, Image Processing, Soft Computing, Fuzzy Logic and Microcontrollers. She has worked in many diverse areas such as Machine Learning, Neural Networks, Medical Image Processing and Computer Graphics. She has published more than 18 papers in various International Journals and Conferences. She is a life member of Indian Society for Technical Education (ISTE), member of the International Association of Engineers (IAENG) and Computer Society of India (CSI). She won the Best Paper award in the International Conference on Novel Issues and Challenges in Science and Engineering'16 (NICSE'16). She is a reviewer of Scopus Indexed journals namely, IAENG International Journal of Computer Science and Journal of Machine Learning Research (JMLR).

Image Enhancement Using the Image Sharpening, Contrast Enhancement, and Standard Median Filter

Krishna S. S.

M. Tech Student, Department of Computer Science and Engineering, Lourdes Matha College of Science and Technology, Trivandrum, Kerala, India
krishnamalu53@gmail.com

Asha A. S.

Associate Professor, Department of Computer Science and Engineering, Lourdes Matha College of Science and Technology, Trivandrum, Kerala.
Asha.AS@lmcst.ac.in

***Abstract*—I explained the three methods of image enhancement: Image Sharpening, Contrast Enhancement and Standard Median Filtering where noise is filtered using these methods first and finally noise is eliminated. The proposed algorithm consists of three distinct stages. Image enhancement processes consist of a collection of techniques that seek to improve the visual appearance of an image or to convert the image to a form better suited for analysis by a human or a machine. In un sharp masking filter function is used sharpening the image sharpening techniques are designed to enhance the high-frequency aspects of the image. High-frequency aspects, such as edges around major features of the image, are particularly desirable to sharpen to improve the visual appearance of the image. In final stage apply the median filter to suppress noise amplification and produce the more enhanced output. The performed computer experiments on different low contrast images demonstrated the efficiency of the proposed algorithm in processing synthetic and real degraded images, as it provided better and clearer results when compared to several existing contrast enhancement algorithms. The median filter is an effective method for the removal of impulse based noise on images. This is due to the partial averaging effect of the median filter and its biasing of the input stream, rather than straight mathematical averaging.**

***Index Terms*—Enhancement, Un sharp Masking, Median Filter.**

I. INTRODUCTION

Over the last decades, substantial progress has been made in the fields of digital image processing and computer vision by both professionals and researchers. Contrast enhancement is an important image processing field that plays an essential role in improving the visible quality for a variety of image-related applications. Moreover, it is considered an important processing step in different scientific applications.

A median filter is nonlinear type of filter and efficient to remove of salt and pepper noise and Gaussian noise. It helps to keep the sharpness of the image at the time of removing the noise. Potency of median filter depends on the scale of the windowing. For mammography 3X3 window provides smart result. In median filter, the value of an output component is determined by the

median of the neighborhood pixels. The median is good to evaluate extreme values and so better able to take away this outlier without reducing the sharpness of the image.

The low-contrast effect reduces the visual quality of an image and thus, it should be handled properly to provide acceptable quality for digital images. Hence, it is desired to redistribute the intensities of a given image to the entire dynamic range in order to improve its contrast and provide an adequate representation for its information.

Generally, the methods for contrast enhancement of can be categorized into direct and indirect methods. In the direct methods, a certain contrast term is used to define the image contrast. Since a digital image contains simple and complex patterns, using such contrast terms may fail to measure the contrast in a variety of images. On the contrary, indirect methods try to improve the image contrast by redistributing the probability density. This means that the intensities of a given image can be reallocated within the natural range without using a certain contrast term.

Most of these methods are implemented either in the spatial domain or the frequency domain. Accordingly, the image is processed as it is in the spatial domain, whereas in the frequency domain, the image is first transformed to its frequency version, then the processing occurs; after that, an inverse transformation is applied to view the image in the spatial domain. Histogram-based methods for contrast enhancement are the most famous indirect methods due to straightforward implementation. Despite the major advantages of these indirect methods, many of such tend to produce undesirable degradations (e.g. under-saturation, over-saturation) to the processed images. Hence, a low-complexity algorithm is introduced in this article to process low contrast images rapidly and efficiently without introducing any undesirable degradations.

In addition, most of the available contrast enhancement methods that provide acceptable results have a complex structure with a high number of calculations. However, it is a simple structure and does not utilize the concept of histogram equalization. To test the processing ability of the proposed method, various computer experiments on different low-contrast images are performed.

II. METHODS

A. Histogram Equalization

Intensity value adjustment process can be done automatically by using the histogram equalization. Histogram equalization involves changing the intensity values so that the histogram of the output image approximately matches the histogram specified. This technique

is often used for processing the histogram is the histogram equalization (HE) which to produce a histogram uniform or evenly so it is often also called flattening histogram, This technique can be done once for the entire image areas (global histogram equalization) or with several times repeated for each image blocks (sub-image).

Equation 1 is used to perform a histogram equalization process.

$$H(b_k) = \sum_{i}^{k} \frac{S_i}{S} = \sum_{i}^{k} p_{k(b_k)}, \quad \begin{matrix} 0 \le b_k \le 1 \\ k = 0,1,\ldots, L-1 \end{matrix}$$

$$b_k = \frac{k}{L-1}, 0 \le k \le L-1$$

Steps in using the histogram equalization:

a. The value of the gray level image and a constituent.

b. Calculate the maximum value of the gray level image results. Histogram will determining the histogram equalization.

c. From the original image histogram, Save frequency degrees of gray in the array (vector). Set array (vector) whose size depends on the maximum degree value. Then, degrees of gray in the position vector compute frequency.

d. Create the histogram equalization. Histogram equalization was obtained by calculating the degree of gray emergence presentation that is multiplied by the maximum gray level of the original image.

e. Find the value of gray level of the new image results by using histogram equalization.

f. To map the image histogram equalization becomes a new one, empty matrix is equal to the size of the original image. The value of a matrix based on the image.

Histogram is a useful tool to analyze the brightness and contrast of an image. It shows how the intensity values of an image is distributed and the range of brightness from dark to bright. An image can be enhanced by remapping the intensity values using the histogram. Also, histogram is used to segmentize an image into the several regions by thresholding. For example, if the image intensities in the histogram are divided into 2 groups, the threshold value can be chosen at the middle of 2 peaks in the histogram.

Images captured with insufficient illumination generally have dark shadows and low contrast. This problem seriously affects other forms of image processing schemes

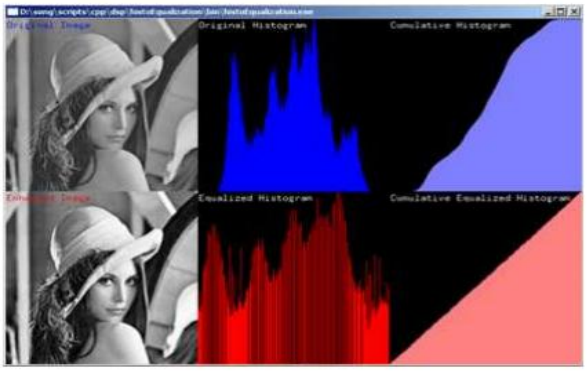

Fig.1. A screenshot of an example of histogram equalization

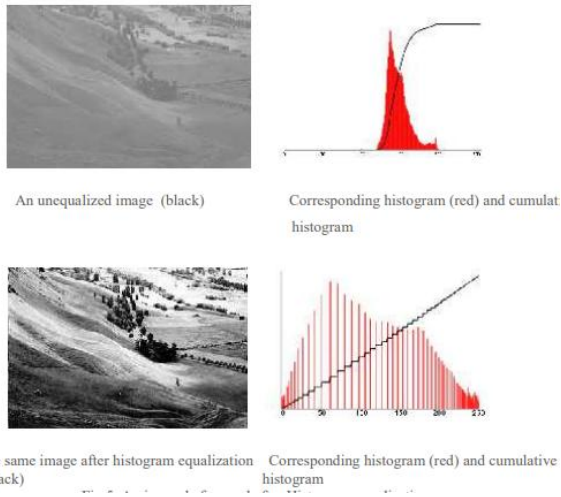

Fig.2: An image before and after Histogram Equalisation.

such as face detection, security surveillance and image fusion. A new image enhancement algorithm using the important features of the contourlet transform has been presented by Asmare et al. A new transformation function is developed based on the existing sigmoid function and the tanh functions which have very interesting properties in enhancing images which are suffering from low illuminations or non-uniform lighting conditions. Literature dictates that contourlet transform has better performance in representing the image salient features such as edges, lines, curves, and contours than wavelets for its anisotropy and directionality and is therefore well suited for multiscale edge-based image enhancement. The algorithm works for gray scale and color images. For a color image, it is first converted from RGB (red, green, and blue) to HSI (hue, saturation, and intensity) color model. Then, the intensity component of the HSI color space is adjusted the preserving the original color using a new nonlinear transformation function. The simulation results show that this approach gives encouraging results for images taken in low-light and/or non-uniform lighting conditions. The results obtained are compared with other enhancement algorithms based on wavelet transform, curvelet transform, bandlet transform, histogram equalization (HE) and contrast limited adaptive histogram equalization. The performance of the enhancement based on the contourlet transform method is superior.

B. Image Sharpening

Image sharpening techniques are designed to enhance the high-frequency aspects of the image. High-frequency aspects, such as edges around major features of the image, are particularly desirable to sharpen to improve the visual appearance of the image. In principle, image sharpening consists of adding to the

original image a signal that is proportional to a high-pass filtered version of the original image. Value high-pass filtered and added to the original image data, which results in improved edge and noise amplification. Image sharpening refers to any enhancement technique that highlights edges and fine details in an image. Image sharpening is widely used in printing and photographic industries for increasing the local contrast and sharpening the images.

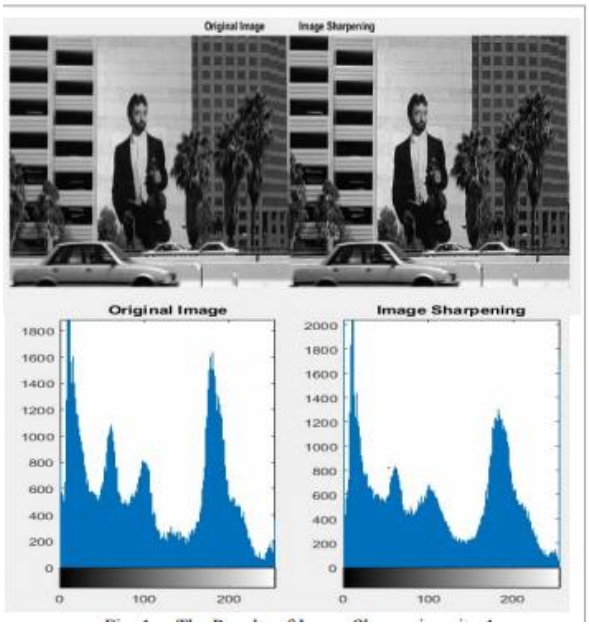

Fig. 3: The Results of Image Sharpening citra1

C. Noise Removal Noise

Removal is techniques used to eliminate distractions that exist in an image. In this experiment, the noise is removed in the form of Salt and Pepper (the type of noise that contains bright spots and dark in an image). One of the methods used in the noise removal process, Standard Median Filter (SMF). SMF is a method of filter is used to suppress impulse noise by blurring the fine line detail and then overwrite it with the median pixel next to it.

A median filter is nonlinear type of filter and efficient to remove of salt and pepper noise and Gaussian noise. It helps to keep the sharpness of the image at the time of removing the noise. Potency of median filter depends on the scale of the windowing.

For mammography 3X3 window provides smart result. In median filter, the value of an output component is determined by the median of the neighborhood pixels. The median is good to evaluate extreme values and so better able to take away this outlier without reducing the sharpness of the image.

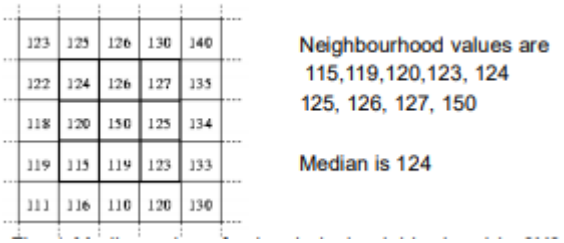

The median filter is order statistics filter most used in image processing. The minimum and maximum intensity values of all the elements inside a windowed region. If the intensity of the central element lies inside the intensity vary

unfold of its neighbors, it is passed on to the output image with out changing the intensity. However, if the central element intensity is larger than the utmost worth, it is s set up to the utmost maximum value; if the central element intensity is a smaller amount than the minimum value, it is set up to the minimum value.

CONCLUSION

In this paper, image quality improvements have been tested using a contrast enhancement, sharpening and noise reduction. The proposed a contrast enhancement system for image sequences which can enhance contrast with suppressing undesired noise amplification based on median filtering processing. Image Sharpening has good results for this topic because it isn't change information or pixel, it's close to the original image information.

REFERENCES

[1] T. Arici, S. Dikbas and Y. Altunbasak, "A histogram modification framework and its application for image contrast enhancement", IEEE Transactions on Image Processing, vol. 18, no. 9, pp. 1921-1935, 2009.

[2] A. Beghdadi and A. le Negrate, "Contrast enhancement technique based on local detection of edges", Computer Vision, Graphics, and Image Processing, vol. 46, no. 2, pp. 162-174, 1989.

[3] H. Cheng and H. Xu, "A novel fuzzy logic approach to contrast enhancement", Pattern Recognition, vol. 33, no. 5, pp. 809-819, 2000.

[4] S. Huang, F. Cheng and Y. Chiu, "Efficient contrast enhancement using adaptive gamma correction with weighting distribution", IEEE Transactions on Image Processing, vol. 22, no. 3, pp. 1032-1041, 2013.

[5] R. Sherrier and G. Johnson, "Regionally adaptive histogram equalization of the chest", IEEE Transactions on Medical Imaging, vol. 6, no. 1, pp. 1-7, 1987.

[6] A. Polesel, G. Ramponi and V. Mathews, "Image enhancement via adaptive unsharp masking", IEEE Transactions on Image Processing, vol. 9, no. 3, pp. 505510, 2000.

[7] Z. Al-Ameen, G. Sulong and M. Johar, "Employing a suitable contrast enhancement technique as a prerestoration adjustment phase for computed tomography medical images", International Journal of Bio- Science and Bio-Technology, vol. 5, no. 1, pp. 73-80, 2013.

[8] Y. Kim, "Contrast enhancement using brightness preserving bi-histogram equalization", IEEE Transactions on Consumer Electronics, vol. 43, no. 1, pp. 1-8, 1997.

[9] M. Mahamdioua and M. Benmohammed, "New meanvariance gamma method for automatic gamma correction", International Journal of Image, Graphics and Signal Processing, vol. 9, no. 3, pp. 41-54, 2017.

[10] A. Raju, G. Dwarakish and D. Reddy, "A comparative analysis of histogram equalization based techniques for contrast enhancement and brightness preserving", International Journal of Signal Processing, Image Processing and Pattern Recognition, vol. 6, no. 5, pp. 353-366, 2013.

[11] N. Hassan and N. Akamatsu, "A new approach for contrast enhancement using sigmoid function", International Arab Journal of Information Technology, vol. 1, no. 2, pp. 221-225, 2004.

[12] A. Łoza, D. Bull, P. Hill and A. Achim, "Automatic contrast enhancement of low- light images based on local statistics of wavelet coefficients", Digital Signal Processing, vol. 23, no. 6, pp. 1856-1866, 2013.

[13] M. Nilsson, M. Dahl and I. Claesson, "The successive mean quantization transform", IEEE International Conference on Acoustics, Speech, and Signal Processing; 23-23 March; Philadelphia, USA, pp. 429-432, 2005.

Krishna S S is currently doing her M. Tech degree in Department of Computer Science and Engineering, Lourdes Matha College of Science and Technology, Trivandrum, Kerala, India. She had secured B. tech from PRS college of engineering and Technology. Contact mail: krishnamalu53@gmail.com

Prof. ASHA A S is currently the Associate Professor in CSE department, LMCST. She had secured B. tech degree from College of Engineering Kidangoor, Kottayam and ME from Govt College of Engineering Tirunelveli. Two publications and two conference proceedings are in her credit. Her area of specialization- Data Structures and algorithms, Operating systems, programming in C/C++, Software Engineering

Novelty in Image Enhancement through Zooming and Reconstruction

Nisha J William,
M.Tech Student, Department of Computer Science and Engineering,
Lourdes Matha College of Science and Technology, Trivandrum, Kerala, India
nishajwilliam@gmail.com

Nisha O S
Assistant Professor, Department of Computer Science and Engineering,
Lourdes Matha College of Science and Technology, Trivandrum, Kerala, India
nisha.os09@gmail.com

***Abstract*— As we know image processing is in vogue, image enhancement technique has become favourite research field recently. Image quality is of have widespread importance in several areas of image application such as biometric verification, medical field, satellite imaging, underwater imaging, etc. This requires image obtained to be sharp and clear without any artifacts. Moreover, on zooming, it should remain clear. Thus, focusing on these points, this paper proposes an algorithm which gives a novel image enhancement technique via zooming and reconstruction to improve image quality. With this technique, Discrete Wavelet Transform has been adopted in combination with an interpolation methodology to zoom the image into larger size. The blurriness and noise contained in image is removed by Lucy-Richardson Deconvolution algorithm. Further, contrast enhancement is also practised to improve image glare using CLAHE. Improvement in image quality can be assessed by comparing PSNR values of original image and output image. Proposed technique is a better approach to provide good quality zoomed images.**

***Keywords*— Enhancement, Wavelet Transform, Interpolation, Deconvolution, Contrast Equalization.**

I. INTRODUCTION

AS we are living in the age of digital techniques, it is obvious that, processing of image signal digitally will be much more preferred in order to exploit the processing capabilities of computers. The technique of processing image signal using computer algorithms is known as digital image processing. The most important digital image processing technique is image enhancement which refers to accentuation or sharpening of image features such as edges, boundaries, or contrast to make a graphic display more useful for display and analysis. The enhancement process does not increase inherent information content in data rather it increases dynamic range of chosen features so that they can be detected easily. Image enhancement technique includes gray level and contrast manipulation, noise reduction, edge crispening and sharpening, filtering, interpolation and magnification, pseudo colouring, and so on. There is no general unifying theory of image enhancement at present because there is no general standard of image quality that can serve as design criteria for an image enhancement system.

The aim of image enhancement is to improve the interpretability or perception of information in images for human viewers, or to provide `better' input for other automated image processing systems. Generally, on zooming images it will appear to show poor quality due to low resolution. To solve this problem, this paper introduces an effective method to enhance images by reconstructing it after zooming. The image will be divided into four sub-bands and operations will be applied on each band separately. Interpolation is the technique used here for zoom the image. Blurriness and noise in image are then removed and image is then

adjusted with histogram equalization for contrast improvement.

This paper is organized as follows. Section II provides an overview of previous research on various image enhancement techniques. Section III depicts the methods used in this paper and explanation for choosing the specific technique. Detailed descriptions of different enhancement techniques used in this paper are discussed in Section IV. Section V illustrates step by step working of the proposed algorithm and Section VI concludes the paper.

II. LITERATURE SURVEY

The methodology to change digital interpolated images at higher resolution is available today. As this field was growing more and more important, a method for image enhancement using DWT and CLAHE was introduced by Archie & Himanshu [1]. A comparative study of 2D image processing in gray scale using wavelets was made by Jose Alfredo Acuna-Garcia *et al*. [2] to understand the information that can result from Discrete Wavelet Transform of an image in 2D in grayscale, using kernel Wavelet Daubechies. Chadda *et al.* [3] presented a survey on different zooming techniques used for digital images. A survey on methods for construction of super resolution images was discussed by Olivier & Hanqiang [4].

Abirami *et al.* [5] practiced the combination of the wavelet transforms and various interpolation algorithms with different approaches for zooming that included still objects or moving objects. Sharma & Swami [6] then introduced a new redundant wavelet RWT and used it in combination with bi-cubic interpolation to yield better outcomes. These researches were extended for shearlet based iterative refinement representation by Lakshman [7] and with sparsity priors b Lim [8].

On the basis of these researches, Saranya *et al.* [9] made a survey on wavelet domain techniques that are used for super resolution of images. Sinha *et al* [10] presented an analysis on performance of high resolution images formed with different interpolation techniques in multimedia communication systems. Tripathi & Kirar [11] studied and compared various image enhancement techniques introduced till now based on their experimental values and performance analysis. A new approach to image enhancement was analyzed by Gayakwad & Ravishankar [12] that took into account the glare and contrast of the image using histogram specification apart from its size.

Further, Kekre *et al* [13] introduced a hybrid watermarking technique using SVD which proved to be better and finally, Suresha & Prakash [14] implemented a natural super resolution technique using modified adaptive bilinear interpolation combined with contra harmonic mean and adaptive median filter in spatial domain. Image Contrast Enhancement using combination of DWT & SWT with CLAHE were made by Rachit Kumar *et al*. [15]. Vidhya Ganesh and H Ramesh [16] were analyzed the effectiveness of CLAHE on Multispectral Satellite Imagery to study its effectiveness in different regions of the electromagnetic spectrum.

Review on various recently used image enhancement techniques were discussed by Ravinder Kaur *et al*. [17]. RupneetKaur Hanspal *et al*. [18] presented a brief study on image enhancement techniques such as Histogram Equalization, Adaptive Histogram Equalization, Contrast Limited Adaptive Histogram Equalization and Exact Histogram Equalization. Kuldeep Narayan Shukla *et al*. [19] provide an overview and analysis of different techniques commonly used for image enhancement.

The deduced methods till date has outperformed well in producing better quality images; but cannot be used in the long run for getting a sharper, super-resolution images. On zooming images it suffers lack of clarity and poor resolution. Also it shows blurred effect on

zoomed images. Therefore, keeping these technical gaps in mind, it is observed that there is an urgency to design a novel image enhancement strategy that produces best quality image on zooming without blurriness and also deals with the contrast of an image after zooming apart from just the details contained in it.

III. METHODOLOGY

In the proposed algorithm, a novel technique is postulated for image zooming, which combines the methods of Discrete Wavelet Transform (DWT) with Spline interpolation technique. DWT is considerably easier to implement when compared to other wavelet transforms like FWT, CWT, etc. The DWT fails often to provide a good quality image as it distorts images at fewer points, generally at the corners. Therefore, in order to remove distortion related issues, interpolation techniques are combined with DWT; by virtue of which the image is improved to a greater extent.

Image interpolation is used to resize or zoom the image to increase the quantity of pixels, so that when an image is zoomed more details in it can be seen. Different types of interpolation techniques include spline, cubic, bi-cubic, nearest neighbour, linear, bilinear etc. Of these techniques, Spline interpolation comes out to be better since it take into consideration a larger domain of pixels.

To remove blurriness in zoomed image, Lucy-Richardson Deconvolution Algoritm is applied. It is an iterative procedure for recovering an underlying image that has been blurred by a known point spread function. It works on small areas in image, called tiles, as opposed to the whole image. Zoomed images will be then free from blurriness or noise.

In addition to enhancement, the proposed technique also improves the contrast of the image which further adds to the image quality. Contrast Limited Adaptive Histogram Equalization (CLAHE) is the technique used here to improve contrast in images. CLAHE method is very useful where the brightness requirement is high like as in geographical channels or underwater environments. CLAHE is an advancement of Adaptive Histogram Equalization (AHE) technique. AHE has a drawback of over amplifying noise. CLAHE is equipped to limit the over amplification by clipping the histogram at a predefined value (called clip limit) before computing the CDF.

Image quality assessment can be evaluated using methods such as peak signal to noise ratio (PSNR), visual signal to noise ratio (VSNR), most apparent distortion (MAD), visual information fidelity (VIF), SSIM and gradient based similarity index, etc. Of these, PSNR is the measure we have adopted in this paper. It is the conventional full reference image quality assessment method which calculates pixel-wise distances between distorted image and reference image.

IV. ENHANCEMENT TECHNIQUES

A. *Discrete Wavelet Transform (DWT)*

Discrete Wavelet Transform (DWT) has been introduced as a highly efficient and flexible method for sub band decomposition of signals. It divides the image into 4 sub-bands which can be evaluated individually using different set of values applied on each band. The sub-bands are usually low and high filters, *i.e.*, *LL*, *LH*, *HL* and *HH*, where *'L'*, *'H'* denotes low and high filters, respectively. The low pass tells averaging group of pixels, whereas high pass stores error of low passes. Thus, the output image of *DWT* is shown in Fig. 1.

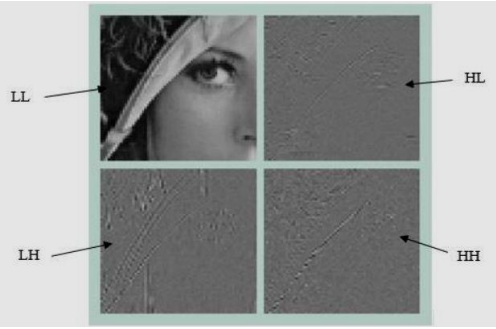

Fig. 1. Output Image of DWT

The inverse DWT is applied to reconstruct original wavelet. Just as a forward transform used to separate the image data into various classes of importance, a reverse transform is used to reassemble the various classes of data into a reconstructed image. The filtering procedure is just the opposite - we start from the topmost level, apply the filters column wise first and then row wise, and proceed to the next level, till we reach the first level.

Haar wavelet is used along with DWT. For an input represented by a list of numbers, the Haar wavelet transform may be considered to simply pair up input values, storing the difference and passing the sum. This process is repeated recursively, pairing up the sums to provide the next scale, finally resulting in differences and one final sum.

B. Spline Interpolation

Image interpolation is used to resize or zoom the image from one pixel grid to another by increasing the total number of pixels. Zooming increases the quantity of pixels, so that after zooming of an image, you will see more detail. Interpolation works by using known data of neighbouring pixel points to estimate values at unknown points. Image interpolation works in two directions, and tries to achieve a best approximation of a pixel's color and intensity based on the values at surrounding pixels. Fig. 2 illustrates how resizing / enlargement works.

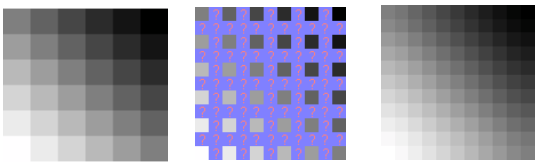

(a) (b) (c)

Fig. 2. Spline Interpolation (a)Original Image (b)Before Interpolation (c)After Interpolation

Spline interpolation retains the most image information after an interpolation. Unlike cubic convolution, the cubic B-spline kernel is not interpolatory since it does not satisfy the necesssary constraint that h(0)=1 and h(1)=h(2)=0.This positivity of the B-spline kernel is attractive for our image processing application.

C. Lucy-Richardson Deconvolution Algorithm

The Richardson–Lucy algorithm, also known as Lucy–Richardson deconvolution, is an iterative procedure for recovering an underlying image that has been blurred by a known point spread function. When an image is produced using an optical system and detected using photographic film or a charge coupled device for instance, it is inevitably blurred, with an ideal point source not appearing as a point but being spread out into what is known as the point spread function. The observed image can be represented in terms of a transition matrix p operating on an underlying image as in Eqn. 1.

$$d_i = \sum_j p_{i,j} u_j \qquad (1)$$

where u_j is the intensity of the underlying image at pixel j and d_i is the detected intensity at pixel i .

D. Contrast Limited Adaptive Histogram Equalization

Contrast Limited Adaptive Histogram Equalization (CLAHE) is an image processing technique used to improve contrast in images. It computes several histograms of an image each corresponds to a distinct section of the image and uses them to redistribute the lightness

values of the image. It is suitable for improving the local contrast and enhancing the definitions of edges in each region of an image.

CLAHE is an advancement of Adaptive Histogram Equalization (AHE). Ordinary AHE has a tendency to over amplify noise in relatively homogeneous regions of an image. Contrast Limited AHE (CLAHE) is a variant of adaptive histogram equalization in which the contrast amplification is limited, so as to reduce the problem of noise amplification. CLAHE limits the amplification by clipping the histogram at a predefined value before computing the Cumulative Distribution Function (CDF). The value at which the histogram is clipped, the so-called clip limit, depends on the normalization of the histogram and thereby on the size of the neighbourhood region. It is advantageous not to discard the part of the histogram that exceeds the clip limit but to redistribute it equally among all histogram bins as shown in Fig. 3.

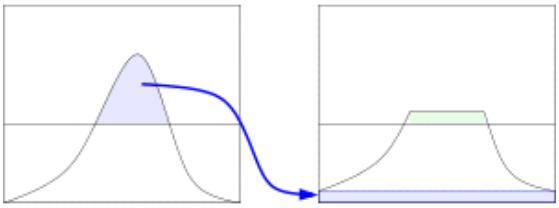

Fig. 3. CLAHE limits amplification by clipping at a predefined value

E. Image Quality Measurement – PSNR

It is necessary to establish quantitative/empirical measures to compare the effects of image enhancement algorithms on image quality. The term Peak Signal-to-Noise Ratio (PSNR) is an expression for the ratio between the maximum possible value (power) of a signal and the power of distorting noise that affects the quality of its representation. It calculates pixel-wise distances between distorted image and the corresponding reference image; i.e. the distorted and the reference images are compared pixel-by-pixel.

Because many signals have a very wide dynamic range, (ratio between the largest and smallest possible values of a changeable quantity) the PSNR is usually expressed in terms of the logarithmic decibel (dB) scale. In general, higher the PSNR value, the analyzed zooming quality will be higher. The PSNR is calculated using Mean Squared Error (MSE). The mathematical representation is given by Eqn. 2 and Eqn. 3.

$$MSE = \frac{b}{kl}\sum_{0}^{k-1}\sum_{0}^{l-1} ||e(k,l)-f(k,l)||^2 \quad (2)$$

$$PSNR = 20\ log_{10}\left(\frac{MAX_e}{\sqrt{MSE}}\right) \quad (3)$$

This can also be represented in a text based format as in Eqn. 4 and Eqn. 5 $MSE = \left(\frac{b}{kl}\right) \times sum(sum((e-f)^2))$ (4) $PSNR = 20 \times log\frac{(max(max(e)))}{((MSE)^{0.5})}$ (5)

where *'e'* represents original image's matrix data, *'f'* is degraded image's matrix data, *'k'* denotes number of rows, *'l'* is number of columns of image and *'MAXe'* is the maximum pixel value.

V. PROPOSED ALGORITHM

The application of DWT is applied using a discrete set of wavelet scales and is translated with predefined rules. The algorithm is a combined method of DWT and Spline interpolation technique and is given as follow:

1. *Start*
2. A ← image
3. Decompose 'A' into four sub-bands say (a1, a2, a3, a4) using *DWT* with 'haar' wavelet
4. *for* i = 1,..,3 // differentiating *R, G, B* colors of each of 4 sub-bands
5. b[i] ← a1(:,:,i)
6. c[i] ← a2(:,:,i)
7. d[i] ← a3(:,:,i)
8. e[i] ← a4(:,:,i)
9. *End for*
10. *for* i =1,..,3 // spline interpolation is applied on each sub-band
11. w1[i] = interpolate(b,i)
12. w2[i] = interpolate(c,i)
13. w3[i] = interpolate(d,i)
14. w4[i] = interpolate(e,i)
15. *End for*

16. *for* i =1,..,3
17. Combine the updated sub-bands into single image using inverse *DWT*
18. *End for*
19. Apply Lucy-Richardson Algorithm(X) //to reduce blurring effect after zooming
20. Apply *CLAHE* (X) // applying contrast equalization on the image
21. Calculate *PSNR* (A) //finding *PSNR* value of input image
21. Calculate *PSNR* (X) //finding *PSNR* value of output image
22. *End*

First of all, an input image is read from the image database and some pre-processing is applied over the image. Further the image is subjected to enhancement process by the four techniques viz. DWT, Spline Interpolation, Lucy-Richardson Deconvolution Algorithm and CLAHE. The RGB input image is divided into its three components: red, green and blue and DWT is applied on each color component seperately. DWT divides image into 4 sub-bands LL, LH, HL and HH where 'L' and 'H' denotes low and high filters. To zoom the image Spline interpolation technique is applied over it which enlarges image size.

The processed image can contain blurriness and noise. To avoid these artifacts Lucy-Richardson Deconvolution Algorithm is applied on image. Thus, resultant image will be free from noise and distortion. Further, with a view to up-grade the glare and contrast of the given image, contrast equalization through CLAHE is adopted. The resulting image can be compared with original image in terms of image statistics PSNR.

VI. CONCLUSION

In this paper, a novel technique is postulated for image zooming and reconstruction, which combines the method of DWT with Spline interpolation. Spline interpolation with DWT comes out to be a better zooming method which enlarges size of image by adding more pixels. In order to remove noise related issues, Lucy-Richarson Deconvolution Algorithm is adopted. Thus, the zoomed images are free from blurriness or noise. The proposed technique also improves contrast of the final image by using CLAHE, which further adds to image quality. When the methods are compared with existing techniques, then to astonishment; it gives better results in terms of PSNR(dB) values.

REFERENCES

[1] Archie Mittal, Himanshu. Jindal, "Novelty in Image Reconstruction using DWT and CLAHE" *I.J. Image, Graphics and Signal Processing*, 2017, 5, 28-34 Published Online May 2017 in MECS

[2] Jose Alfredo Acuna-Garcia, Sandra Luz Canchola-Mag daleno and Fausto Abraham Jacques Garcia "Comparative Study: 2D Image Processing In Gray Scale Using Wavelets", *International Journal of Computer Science and Software Engineering (IJCSSE)*, Volume 8, Issue 7, July 2019

[3] S. Chadda, N. Kaur and R. Thakur, "Zooming Techniques for Digital images: A Survey",‖ I*nternational Journal of Computer Science and Technology* 3(1), 2012

[4] R. Olivier and C. Hanqiang, "Nearest Neighbor Value Interpolation",‖ *International Journal of Advanced Computer Science and Applications* 3(4): 318-321, 2012

[5] A. Abirami, N. Akshaya, D. Poornakala, D. Priyanka, C. R. kumar, "Enhancement of Satellite Image Resolution with Moving Objects",‖ *International Journal of Electronics and Communication Engineering* 4(6),2013

[6] A. Sharma, and P.D. Swami, "Redundant Wavelet Transform based Image Super Resolution",‖ *International Journal of Engineering Research and Applications* 3(4), 2013

[7] H. Lakshman, W. -Q Lim, H. Schwarz, D. Marpe, G. Kutyniok, and T. Wiegand, "Image interpolation using Shearlet based iterative refinement",‖ *International Conference on Image Processing*, IEEE, 2013a

[8] H. Lakshman, W. -Q Lim, H. Schwarz, D. Marpe, G. Kutyniok, and T. Wiegand, "Image Interpolation using Shearlet based Sparsity Priors",‖ *In: The International Conference on Image Processing*, IEEE: 655–659, 2013b

[9] P. Saranya, K. Fatimakani, P. Kanchanadevi, S. Venkatesan and S. Govindaraju, "A Survey on Wavelet Domain Techniques for Image Super Resolution",‖ *International Journal of Computer Science and Mobile Computing*, 2014

[10] A. Sinha, M. Kumar, A. K. Jaiswal, and R. Saxena, "Performance analysis of high resolution images using interpolation techniques in multimedia communication system",‖ *International Journal of Signal Image Processing* 5(2): 39–49, 2014

[11] N. Tripathi, and K. G. Kirar, "Image Resolution Enhancement by Wavelet Transform based Interpolation and Image Fusion",‖ *International Journal of Advanced Research in Computer Science and Software Engineering* 4(8), 2014

[12] S. B. Gayakwad and S. S. Ravishankar, "Image enhancement by Histogram Specification",‖ *International Journal of Recent Advances in Engineering & Technology* 2(4), 2014

[13] H. B. Kekre, Tanuja Sarode, Shachi Natu, "Performance Comparison of Watermarking Using SVD with Orthogonal

Transforms and Their Wavelet Transforms",I *International Journal of Image, Graphics and Signal Processing (IJIGSP) 7(4),* 2015
[14] D. Suresha, H. N. Prakash, "Natural Image Super Resolution through Modified Adaptive Bilinear Interpolation Combined with Contra Harmonic Mean and Adaptive Median Filter",I *International Journal of Image, Graphics and Signal Processing (IJIGSP) 8(2),* 2016
[15] Rachit Kumar, Manan Mehta, Lokesh Rathi, Neelabh Harsh and Mr. Santhosh B, "Image Contrast Enhancement using Combination of DWT & SWT with CLAHE", *International Journal for Research in Applied Science & Engineering Technology (IJRASET)*, Volume 6 Issue V, May 2018
[16] Vidhya Ganesh R and H Ramesh, "Effectiveness of Contrast Limited Adaptive Histogram Equalization Technique on Multispectral Satellite Imagery", *International Conference on Video and Image Processing (ICVIP)*, December 2017
[17] Ravinder Kaur, Taqdir, "Image Enhancement Techniques- A Review", *International Research Journal of Engineering and Technology (IRJET)*, Volume: 03 Issue: 03 | March-2016
[18] Rupneet Kaur Hanspal, Kishor Sahoo, "A Survey of Image Enhancement Techniques", *International Journal of Science and Research (IJSR),* Vol 6 Issue 5, May 2017
[19] Kuldeep Narayan Shukla, Anjali Potnis and Prashant Dwivedy, "A Review on Image Enhancement Techniques", *International Journal of Engineering and Applied Computer Science (IJEACS)*, Volume: 02, Issue: 07, July 2017

AUTHORS

Nisha J William is an M.Tech student in Computer Science and Engineering from Kerala Technological University. Her area of interest includes Image Processing, Cloud Computing and Big Data. She received her Bachelor's degree in Computer Science and Engineering from Kerala University in 2018. Contact her at: nishajwilliam@gmail.com.

Nisha O.S. obtained her Bachelor's degree in Information Technology from University of Calicut. She obtained her Master's degree in Computer Science and Engineering from Anna University and now she is doing PhD in Computer Science from Noorul Islam University. Currently, she is an Assistant Professor at the Faculty of Computer Science and Information Technology, Lourdes Matha College of Science and Technology, Trivandrum, Kerala. Her specializations include Embedded Systems, VLSI Architecture etc.

Analysis of Balancing of an Inverted Pendulum using PID Controller and a brief Survey on its Control

Revthy A. S.

P.G.Scholar in Control System, *Lourdes Matha college of Science & Technology, Thiruvananthapuram , India;*

revathythejas@gmail.com

Johnson Y.

Associate Professor and HOD, Electrical and Electronics, Lourdes Matha college of Science and Technology, Thiruvananthapuram, India;

johnson.y@lmcst.ac.in

***Abstract*-The present paper aims to balance an inverted pendulum by moving a cart along a horizontal track. A suitable control algorithm is developed for the present problem. Conventional control algorithm like PID is applied and is checked the performance and stability characteristics. The comparison of signals between the potentiometer (sensor) and the reference is done and the error obtained is used to drive the system through the developed controller. System stability characteristics are drawn using MATLAB. The experimental performance of the classical controller will be done by creating a suitable hardware platform.**

INTRODUCTION

THE one-dimensional swinging inverted pendulum with two degrees of freedom (i.e. the angle of the inverted pendulum and the movement of robot along forward and backward direction) is a popular demonstration of using feedback control to stabilize an open-loop unstable system. As a common benchmark for the investigation of automatic control techniques, most of them have been used linearization theory in their control schemes, since the system is inherently nonlinear. In this system, an inverted pendulum is attached to a cart equipped with a motor that drives it along a horizontal track.

The thin vertical rod (the pendulum) hinged at the bottom, referred to as pivot point is mounted on a mobile toy car which can move along horizontal direction. The car, depending upon the direction of the deflection of the pendulum (the angle of the inverted pendulum, Ɵ), moves horizontally in order to bring the pendulum to absolute rest in a vertical position. A PID (Proportional Integral and Derivative) controller has been used to generate signal to control the speed and direction of the motor. The only sensor used in this work was a potentiometer (pot), attached to the bottom of the pendulum rod and variation in its resistance causes change in voltage which is then compared with the reference voltage to generate the appropriate control signal. The mathematical expression was established to find the system transfer function based on Newton's second law of

motion. Simulation of the circuit mechanism was obtained by applying MATLAB.

LITERATURE SURVEY

The paper [1] presents control of a rotary inverted pendulum (RIP) by applying a model-free back stepping (MFBS) control technique. The MFBS technique makes use of a normal form of the system model and estimates the unknown dynamics. The stability of the control in the Lyapunov sense is proven. An approach is also proposed to deal with the unknown control coefficient. The equivalence of the control designed with the proposed method to the control designed with the knowledge of the control coefficient is established. The design method is applied to the balance and tracking control of a rotary inverted pendulum (RIP). The control designed with the proposed method is compared with the LQR control in various settings. The proposed control performs as good as or better than the LQR control, but has an advantage of being model-free.

It has been found that for the RIP control problem, in paper [2], a two-loop robust PID controller has been designed for an inverted cart–pendulum system via pole placement technique where the locations of the closed-loop poles are obtained from an LQR design. It is seen that in addition to yielding better responses (because of additional integral action) than this LQR (equivalent to two-loop PD controller) design, the proposed PID controller is robust enough. It is shown that while this LQR design fails, the proposed PID design yields satisfactory responses. The performance and robustness of the PID design have been verified both on simulation and on the experimental set-up.

In paper [3], the swing up strategy is designed by using trajectory planning and inertia effect such that the pendulum

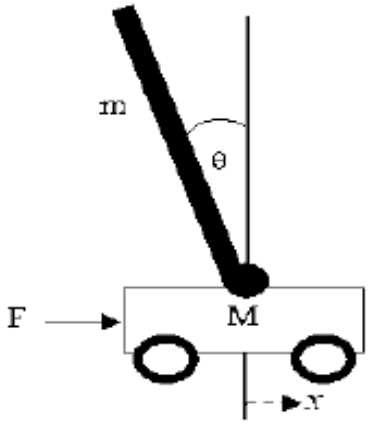

Fig. 1. Cart and Inverted Pendulum System

can be swung to a desired position to trigger the stabilization controller, and the stabilization scheme is implemented by resorting to the nonlinear adaptive Neural Network (NN) control method and Linear Matrix Inequality (LMI) technique. By using Lyapunov stability theory, it can be proved that the target trajectory can be boundedly tracked by the arm section,

and the pendulum section can be balanced in the up-right position with a small error. Finally, two experiment results are respectively given to show the effectiveness of the proposed swing up and stabilization methods.

In paper [4], a dynamic model of a mobile wheeled inverted pendulum (MWIP) system is improved considering friction forces, and a nonlinear disturbance observer (NDO)-based dynamic surface controller is investigated to control the MWIP system. Based on the improved dynamic model of the MWIP system, novel global coordinate transformation was proposed to achieve the DSC control of an MWIP system. Using a coordinate transformation, this non-Class-I type underactuated system is presented as a semi-strict feedback form, which is convenient for dynamic surface controller design. To compensate for parametric uncertainties in a real MWIP-based robot system as well as external disturbances, a dynamic surface controller together with an NDO is designed to stabilize the under actuated plant. The stability of the closed-loop MWIP system is proved by Lyapunov theorem and then combined the proposed DSC controller with NDO. Experimental results are presented to illustrate the feasibility and efficiency of the proposed method.

In paper [5], adaptive model reference control and NN based trajectory planner have been designed on WIP systems for dynamic balance and motion tracking of desired trajectories. The dynamics of the subsystem consisting of the pendulum tilt angle and the mobile platform yaw angle has been shaped to follow a reference model, which is derived by using the LQR optimization technique to minimize both the motion tracking error and the transient acceleration for the best driving comfort. Adaptive control has then been developed using variable structure method to ensure the reference model to be exactly matched in a finite-time horizon, even in the presence of various internal and external uncertainties. The minimized yaw and tilt angular accelerations help to enhance the vehicle rider's comfort. The forward velocity of the unactuated subsystem is made to track the desired motion by suitably designing a reference trajectory for the tilt angle, which directly affects the forward velocity. The stability and optimal tracking performance have been rigorously established by theoretical analysis. The proposed control method considers the presence of various uncertainties, including both parametric and functional uncertainties. In addition, simulation studies have been carried out to demonstrate the efficiency of the developed AGICT and optimized adaptive controller. The simulation results have demonstrated the efficiency of the proposed method.

III. METHODOLOGY

A. System Dynamics Modeling of Inverted Pendulum

An inverted pendulum is a pendulum that has its center of mass above its pivot point. It is unstable and without additional help it will fall over. It can be suspended stably in this inverted position by using a control system to monitor the angle of the pole and move the pivot point horizontally back under the center of mass when it starts to fall over, keeping it balanced. The inverted pendulum is a classic problem in dynamics and control theory and is used as a benchmark for testing control strategies. It is often implemented with the pivot point mounted on a cart that can move horizontally under control of an electronic servo system as shown in Fig.1. This is called a cart

and pole apparatus.

In order to stabilize a pendulum in this inverted position, a feedback control system can be used, which monitors the pendulum's angle and moves the position of the pivot point sideways when the pendulum starts to fall over, to keep it balanced. The inverted pendulum is a classic problem in dynamics and control theory and is widely used as a benchmark for testing control algorithms. Variations on this problem include multiple links, allowing the motion of the cart to be commanded while maintaining the pendulum, and balancing the cart-pendulum system on a see-saw. The inverted pendulum is related to rocket or missile guidance, where the center of gravity is located behind the center of drag causing aerodynamic instability. The understanding of a similar problem can be shown by simple robotics in the form of a balancing cart. Balancing an upturned broomstick on the end of one's finger is a simple demonstration, and the problem is solved by self-balancing personal transporters.

In order to obtain the system dynamics, the following assumptions have been made:

1. The system starts from an equilibrium state i.e. that the initial conditions are assumed to be zero.

2. The pendulum does not move more than a few degrees away from the vertical to satisfy a linear model.

3. A step input (displacement of the pendulum, Θ) is applied to the system.

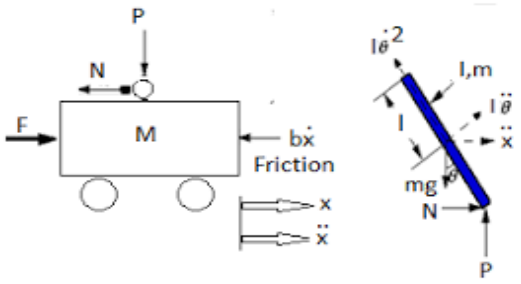

Fig. 2. Free body diagram (FBD) of the inverted pendulum

In the force distribution of the mechanism, while the pendulum rod tilts with some angle, it resolves two force components along horizontal and vertical direction. 'P' denotes the force exerted by the pendulum in vertical direction, and 'N' in horizontal direction, when Θ = 90º, N= 0, and P = maximum.

From the FBD, summing the forces of the cart along horizontal direction, following equation of motion was obtained:

$$M\ddot{x} + b\dot{x} + N = F \qquad (1)$$

Summing the forces in the FBD of the pendulum in the horizontal direction

$$N = m\ddot{x} + ml\ddot{\theta}\cos\theta - ml\dot{\theta}^2\sin\theta \qquad (2)$$

After substituting (2) into (1), the first equation of motion for the system was found as follows:

$$(M+m)\ddot{x} + b\dot{x} + ml\ddot{\theta}\cos\theta - ml\dot{\theta}^2\sin\theta = F \qquad (3)$$

To acquire the second equation of motion, the forces along the perpendicular direction of the pendulum was summed up and found the following equation:

$$P\sin\theta + N\cos\theta - mg\sin\theta = ml\ddot{\theta} + m\ddot{x}\cos\theta \qquad (4)$$

To get rid of P and N terms from (4), the moments around the centroid of the pendulum was taken which resulted following equation:

$$-Pl\sin\theta - Nl\cos\theta = i\dot{\theta} \quad (5)$$

Combining (4) and (5), the second dynamic equation was obtained as follow

$$(i+ml^2)\ddot{\theta} + mgl\sin\theta = -ml\ddot{x}\cos\theta \quad (6)$$

Where $\Theta = \pi$. Assume that, $\Theta = \pi + \phi$ (ϕ represents a small angle from the vertical upward direction).

After linearization the following two equations of motion were obtained.

$$\begin{aligned}(i+ml^2)\ddot{\phi} - mgl\phi &= ml\ddot{x} \\ (M+m)\ddot{x} + b\dot{x} - ml\ddot{\phi} &= u\end{aligned} \quad (7)$$

To obtain the transfer function of the system analytically, the Laplace transforms of the system equations were taken:

$$(i+ml^2)\phi(s)s^2 - mgl\phi(s) = mlX(s)s^2 \quad (8)$$

From (8), the required transfer function obtained as

$$\frac{\phi(s)}{U(s)} = \frac{\frac{ml}{q}s}{s^3 + \frac{b(i+ml^2)}{q}s^2 - \frac{(M+m)mgl}{q}s - \frac{bmgl}{q}} \quad (9)$$

where $q = [(M+m)(i+ml^2) - (ml)^2]$

B. Simulation Analysis using the Controller

Based on the modeling presented in section III.A, the transfer function connecting the angular displacement from the vertical upward direction and the input is numerically modeled as shown in (10) based on the physical data from Table.1. The system consists of an inverted pole hinged on a cart which is free to move in the *x* direction.

Table. 1: Parameters of the inverted pendulum

M	mass of the cart	0.3 kg
M	mass of the pendulum	0.2 kg
B	friction of the cart	0.1 N/m/sec
L	length of the pendulum	0.2 m
I	inertia of the pendulum	0.006 $kg.m^2$
F	force applied to the cart	kg.m/s2
G	gravity	9.8 m/s^2
Θ	Vertical pendulum angle	In degree

$$\frac{\phi(s)}{U(s)} = \frac{7.407s}{s^3 + 0.26s^2 - 36.296s - 7.26} \quad (10)$$

A proportional-integral-derivative (PID) controller is a control loop feedback mechanism widely used in industrial control systems. A PID controller calculates an error value as the difference between a measured process variable and a desired set point. The controller attempts to minimize the error by adjusting the process through use of a manipulated variable.

The PID controller algorithm involves three parameters and is accordingly sometimes called three-term control: the proportional, the integral and derivative values, denoted as P, I, and D respectively. P depends on the present error, I on the accumulation of past errors, and D is a prediction of future errors, based on current rate of change. The weighted sum of these three actions is used to adjust the process via a control element such as the position of a control valve, a damper, or the power supplied to a heating element.

In the absence of knowledge of the underlying process, a PID controller has historically been considered to be the most useful controller. By tuning the three parameters in the PID controller algorithm, the controller can provide control action designed for specific process requirements. The response of the

controller can be described in terms of the responsiveness of the controller to an error, the degree to which the controller overshoots the set point, and the degree of system oscillation. Note that the use of the PID algorithm for control does not guarantee optimal control of the system or system stability.

Some applications may require using only one or two actions to provide the appropriate system control. This is achieved by setting the other parameters to zero. A PID controller will be called a PI, PD, P or I controller in the absence of the respective control actions. PI controllers are fairly common, since derivative action is sensitive to measurement noise, whereas the absence of an integral term may prevent the system from reaching its target value due to the control action.

The Proportional Integral Derivative (PID) is a type of feedback controller whose output, a Control Variable (CV), is generally based on the error (e) between some user-defined Reference Point (RP) and some measured Process Variable (PV). Based on the error each element of the PID controller performs a particular action.

MATLAB Simulink is used for simulation of the required system dynamics. The system is simulated in open loop (in fig.3) and with the PID controller in closed loop (in fig.4) conditions. The three critical combination of K_p=50, K_i =10 and K_d =10 results in figure 4.

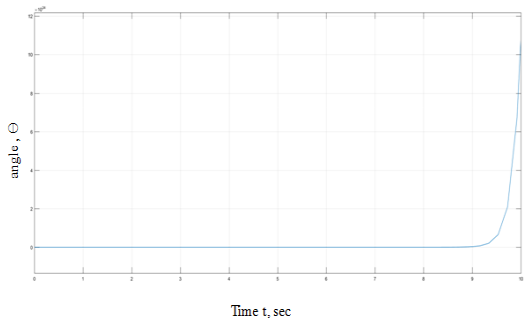

Fig. 3. Open loop Response curve for IP

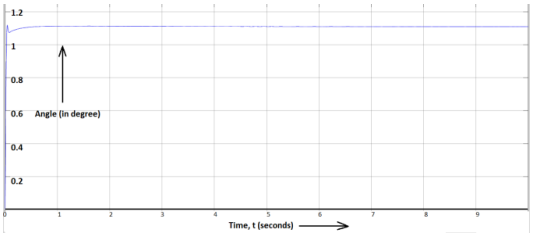

Fig. 4.Closed loop Response curve for IP with controller.

Unstable response is noticed in fig.3. But in fig.4, it is noticed that the response became stable and reaches a condition of stability with moderate steady state error within 1 second.

IV. CONCLUSION

The present paper studied the balancing of an inverted pendulum by moving a cart along a horizontal track with a simulation. The swinging inverted pendulum robot is successfully balanced through the movement of the cart along to and for horizontal direction

using a simple PID controller. The time responses of the system with the PID in closed loop proved its stable response.

REFERENCES

[1] Roberge, J. K., "Control of Rotary Inverted Pendulum Using Model-Free Backstepping Technique," The Mechanical Seal. Bachelor's Thesis, *Massachusetts Institute of Technology*, 1960

[2] A. Ghosh, T.R. Krishnan, B. Subudhi, "Robust proportional–integral–derivative compensation of an inverted cart–pendulum system: an experimental study", School of Electrical Sciences, IIT Bhubaneswar, Orissa Department of Electrical Engineering, NIT Rourkela, Orissa,2011

[3] Xuebo Yang, Member, IEEE, Xiaolong Zheng "Swing up and Stabilization Control Design for an Underactuated Rotary Inverted Pendulum System: Theory and Experiments",2018

[4] Jian Huang, Member, IEEE, Songhyok Ri, Lei Liu, Yongji Wang, Jiyong Kim, and Gyongchol Pak, "Nonlinear Disturbance Observer-Based Dynamic Surface Control of Mobile Wheeled Inverted Pendulum",IEEE TRANSACTIONS ON CONTROL SYSTEMS TECHNOLOGY,2015

[5] Chenguang Yang, Member, IEEE, Zhijun Li, Senior Member, IEEE, and Jing Li "Trajectory Planning and Optimized Adaptive Control for a Class of Wheeled Inverted Pendulum Vehicle Models",IEEE TRANSACTIONS ON SYSTEMS, MAN, AND CYBERNETICS,2014

[6] Jian Huang, Zhi-Hong Guan, Takayuki Matsuno,Toshio Fukuda, and Kosuke Sekiyama "Sliding-Mode Velocity Control of Mobile-Wheeled Inverted-Pendulum []54Systems",IEEE TRANSACTIONS ON ROBOTICS, VOL. 26, NO. 4, 2010

[7] Mahadi Hasan, Chanchal Saha, Md. Mostafizur Rahman, Md. Rabiual Islam Sarker and Subrata K. Aditya, "Balancing of an Inverted Pendulum Using PD Controller",1Industrial Systems Engineering, School of Engineering and Technology, Asian Institute of Technology, Pathumthani, Department of Mechanical Engineering, Rajshahi University of Engineering & Technology, Department of Applied Physics, Electronics and Communication Engineering, Dhaka University,2011

AUTHORS

Revathy A S, from Trivandrum had obtained her B.Tech degree in EEE from Heera college of engineering & technology, Trivandrum. Currently she is doing her M.Tech in Control System in Lourdes Matha College of Science & Technology under KTU.

Dr. Johnson Y, presently working as Associate Professor and HOD in EEE, LMCST, had received his Ph.D in Electrical Engineering (Control Systems) from University of Kerala, M. Tech in Industrial Instrumentation & Control from TKMCE under University of Kerala and B. Tech from M.G. University He also attained Diploma in Management from IGNOU, Microsoft Certified Professional and CISCO Certified Network Associate. His area of interests includes Robust Control, Flight Dynamics, UAV and Satellites. More than 20 papers are under his credit. He bagged Life membership of Kerala Academy of Sciences (KAS) and Institution of Engineers (India) –MIE**.** He is the verified Reviewer in Publons.com with ID publons.com/a/1422443/. He is the recipient of prestigious "**Aerospace Engineering Division Prize**" (for the best research paper published in international journals of Institution of Engineers (India) under Aerospace stream in 2014. He had received CERD Research Fellowship from Govt. of Kerala during 2011 to 2015. He was the National Talent Search Examination (NTSE)-preliminary phase winner in **1993.** Worked as Principal Investigator for some funded Projects from KSCSTE, Govt. of Kerala too.

Wheel chair cum Therapy Unit for Physically Challenged People

Muneera T. N

P.G. Scholar, Applied Electronics and Instrumentation, Lourdes Matha College of Science and Technology Thiruvananthapuram, India
muneeratn@gmail.com

Sajitha P

Assistant Professor, Electronics and Communication, Lourdes Matha College of Science and Technology Thiruvananthapuram, India
sajitha.p@lmcst.ac.in

***Abstract*— The aim of this work is to control a wheelchair by voice of the person who use wheelchairs for their necessities. The proposed system is helpful for elder and handicapped people those who are not able to move themselves. The system also contains a therapy unit that will gives an assistance for limbs of the user which can eliminate numbness due to the continuous rest. An obstacle sensor in the system helps to find the obstacles in the way of movement.**

***Keywords*— Vibrator, Servo Unit**

I. INTRODUCTION

Wheelchair is widely used by aged or physically challenged people. But for using this user needs a self-assistance or they seeks helps from another person. Statistics reveals that 15% of the world population which is about 0.655 billion people are suffering from different sort of physical challenges. Wheel chair controlled by joystick are widely used around the world. But handicapped people those who have issues with finger movement are unable to control the joystick. The proposed system aims to design a wheelchair that can be completely controlled by voice of the user. The system also provides a therapy unit for the user to provide therapy for upper and lower limbs due to continuous rest. The design also consists of an obstacle sensor which helps to avoid obstacles on the way of movement.

II. LITERATURE SURVEY

Design and Development of Smart wheel chair using voice recognition and Head Motion [1] proposed a wheelchair system using head motion and voice recognition. The system detects the head movement by using MEM sensors and given signal to microcontroller

Voice Controlled Wheel Chair for Physically Disabled People [2] put forwards a system for assisting people with physical disabilities and for old aged ones who are not able to move themselves due to their physical weakness. Here voice recognition module is interfaced with DC motors there by the commands from users can be directly used to move the wheelchair system.By using a smart phone wheelchair can be controlled using an app. For detecting obstacles IR sensors are used here.

Design and Construction Of Electric Drive – A smart system for disabled person with therapy facilities [3] introduce a wheelchair system with therapy facilities. It includes a

therapy unit for limbs which uses a vibrator. An ultrasonic sensor is used here for obstacle detection.

Voice Controlled Wheel Chair for Physically Disabled Per- son [4] proposed a system that use users voice commands. The system helps the patient to drive the wheelchair without any ones Help. Wheelchair moves according to the command given by the user . voice recognition is used here by using speech recognition module.

Voice Controlled Wheel chair system [5] introduce a wheelchair system controlled by voice of the person. In this work physically challenged people were assisted by speech recognition technology. Here smartphone is used as an intermediate device.

Wheel Chair for Physically Disabled People with Voice amp;Eye control [6] recommends a concept useful for peoples with loco motor disability. Here wheelchair is controlled by voice commands and eye movement. Eye movement is detected by using a head mounted camera. Output signal corresponding are fed to motor which control wheelchair movement. Voice assistance is also used by this system. By giving proper commands, the movement can be controlled.

Voice based Wheel Chair for Physically Challenged [7] proposed a system which provides assistance for physically handicapped ones those who are not able to move by themselves. It includes a speech recognition module HM2007 with microcontroller and wheelchair. The system provides a mic for the user to give commands HM2007 registers. Motor driver drives the wheel chair according to the commands from microcontroller.

III. METHODOLOGY

A. Existing System

The movement of wheelchair in existing system is con- trolled by using a joystick. Based on the output from joystick, microcontroller give instructions to the motor and wheelchair is moved to the desired location.

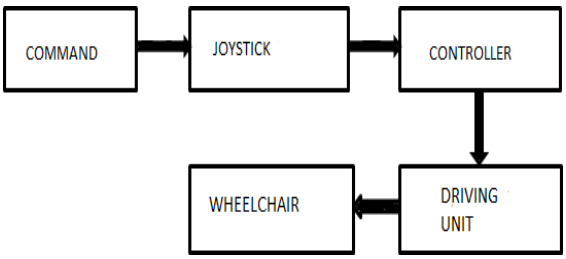

Fig. 1. *Existing system block diagram*

Due to the development of technology, joystick controlled wheelchair are widely available in world. But for physically disabled, handicapped, paralyzed or persons having issues related to fingers or hands, they need hand movement for controlling joystick. Also old aged people those who have poor wrist movement suffer problems while using the joystick. So a surrogate is needed to refute the necessity of joystick for controlling the wheelchair.

B. PROPOSED SYSTEM

The proposed system uses voice commands from the user for operating the wheelchair. But in crowded areas voice can- not be easily recognized. It uses a joystick as an optional one. The system serves as a multipurpose one. It also includes a vibrator and servomotor for preventing numbness experienced due to continuous rest. A switch is used for enabling and disenabling the therapy unit. it consists of a controlling unit and therapy unit.

1) *AT-Mega 2560:* An high performance, 8 bit micro- controller is the master brain of this system. The device can provide output at 16MHZ. The commands from speech recognition device is interpreted by the

microcontroller and turns the wheelchair in the desired location. It can also sense the triggering of therapy unit. It encounters the obstacles in the way of movement and it terminates the motion of wheelchair.

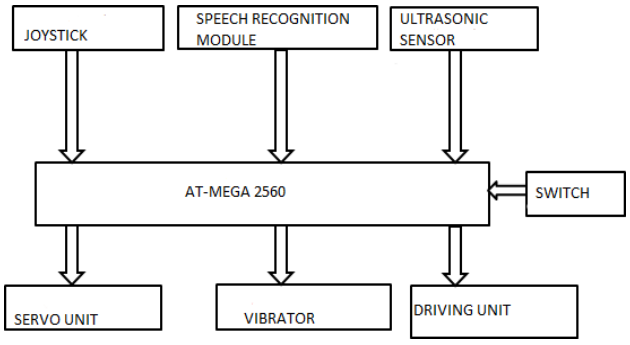

Fig. 2. *Proposed system block diagram*

2) *Joystick:* It works on a simple principle where the machine accepts the hand movement of user with the help of asset of sensors and then converts it into a mathematical code, which finally moves the body in the computer in the desired way. The working principle is simple and is based on vertical and horizontal movements. For moving right and left, horizontal axis is used. Front and back movement is enabled by vertical axis. For moving right and front the value changes from center value to 1024. For moving left and back, the value will lowered to 0 from center value ranges from 540 to 560. Joystick is an innovative device that takes physical movement of human hand and converts the movements for use in a control machines. The output of joystick is analyzed by microcontroller. The device is used here as an optional one in hectic places where the voice cannot be recognized.

3) *Speech Recognition Module:* The entire module is a speaker dependent one. It can support up to 15 voice com- mands in all. Maximum 7voice command would work at the same time. The user only need to train the module first before let it recognize any voice inputs. Voice recognition module used here is V3 module. The module along with a Mic is a board used for feeding input commands. The process starts with the recording of users voice command and copy trained voice to the recognizer. Finally the trained voice command is stored in the flash memory ranging numbers from 0 to 14. When one input command arrives, then V3 module will recognize the command and then it is fed to the microcontroller.

4) *Ultrasonic Sensor:* HC-SR04 is the ultrasonic sensing module used in this system. It can give an accuracy range about 3 millimeter distance. It possess a transmitter emits an ultrasonic waves in one direction and it started timing when it is launched. Ultrasonic speed in the air, would return immediately when it encounters obstacles on the way of its direction. If it detects any obstacle, then a signal is sent to microcontroller and in turn stops the motion of wheel chair.

5) *Driving Unit:* It has four 12 V relays in which each of these are used to make H-Bridge to drive a single motor. It has four n-p-n transistors whose function is to magnify the driving current to drive the relays. Permanent Magnet DC motor is used here. Because it has low cost, high starting torque. A 24V DC lead acid battery is used as power supply unit for the motors.

6) *Servo unit :* HG90 is the servo motor used here. It is actually a DC motor whose speed can be controlled by using gears. Its revolution can be cut off from 90 degree to 180 degree. Rotation of servo motor is limited between the fixed angles. In this system, when hand of the user were placed on the belt attached to the wheel chair, the servomotor enables therapy to the

hands by its to and fro motion which is make easier by the servo motor shaft.

Vibrator: Vibrator is used to provide vibration to the lower limbs, which can suffer numbness due to the continuous rest. It is achieved by constructing a vibrator circuit along with a vibration pad. It helps the patient to regenerate their blood circulation. When a DC current flows through the device it can brings heat from one side and the other side becomes cooler. The therapy unit is the key of this work which have a lot of advantages.

I. CONCLUSION

For disabled and handicapped persons, the proposed system not only helps the locomotion but also provides therapy. The implemented system has a Voice recognition module and Therapy unit. The system helps disabled person can do some kind of therapies without the help of another person. The implemented device helps to improve the lifestyle of the physically disabled persons and lead them to keep pace with others in the society. The system is also able to sense the obstacles, is not present in ordinary wheel chair. In future, for the convenience of the patient the device can be modified and can be implemented as a chair cum bed system. Lastly we can conclude that those people who are socially isolated or lag behind due to their physical disabilities will have the opportunity to move freely without any assistance like other people of the society by using their voice commands.

REFERENCES

[1] Dr.B.Paulchamy, N.Vinothini,S. Sharukhan, S.Sona, M.Sri Gayathri,C.Nandhini.“ Design and Development of Smart wheel chair us- ing voice recognition and Head Motion”.IJSEAS,Volume-3,Issue-5,May 2018.

[2] Priya C A,saadiya,Bagyasree, S D pranjala,Mr.Supreeth H S G.“ Voice Controlled Wheel Chair for Physically Disabled People”.IJRASET,ISSN:2321-.9653, Volume 6, Issue 5,May 2018.

[3] Sania Sheikh,Alfiya Sheikh,Abhishek waghmare,Ankit yadav,Shubham Bhoyar, Chetana Dolase.“ DESIGN AND CONSTRUCTION OF ELEC- TRIC DRIVE –A smart system for disabled person with therapy facilities”IRJET,ISSN(online):2395 0056,Volume:05,Issue:03,March 2018

[4] Prof.Manoj V Bramhe, Navya Vijay, K. Bhagyasree Rao, Payal Bisen,Riddhi Navsalkar, Tanushri Bajganiya.“ Voice Controlled Wheel Chair for Physically Disabled Person”.IJAREEIE,ISSN(print):2320- 3765,ISSN(online):2278-8875,Volume 6, issue 2, February2017.

[5] Mohammad Ilyas Malik,Tanveer Bashir, Mr.Omar Farooq Khan.“ Voice Controlled Wheel chair system”.IJCSMC,Volume 6,Issue 6,June 2017, Pg.411-419.

[6] Prof.Miss.Pranita Bhosale, Mr.Akshay Satpe, Mr. Tapan Singha, Miss.Kajal Patil.“ Wheel Chair for Physically Disabled People with Voice Eye control”. Global Research and development Journal for Engineering. ISSN:2455-5703, Volume 1, Issue 6, May 2016.

[7] Ravi Teja Ch.V, P Shekar, S. Roja, H. Hariprasad, Y. Bhargavi.“ Voice Based Wheel Chair for Physically Challenged”. International Journal of New Innovations in Engineering and Technology. ISSN-2319- 6319,Volume 3, Issue 1, March 2015

Authors

Muneera T N presently working as Assistant Professor, HCET, had received M.tech in Applied Electronics & Instrumentation under APJ Abdul Kalam Kerala technological University and B.tech in Electronics and Communication from under Kerala University. She had published two papers in international journals

Prof. Sajitha P. currently working as Assistant Professor in Dept of ECE, LMCST. She got M. Tech in Applied Electronics and instrumentation from University of Kerala and B.E in Electronics and communication Engineering from M. S UNIVERSITY, Tirunelveli. She has 9 years of teaching experience and 1 year of Industrial Experience in IBM India Pvt limited.

Stair shaped Semicircular Microstrip Patch Antenna Loaded with CSRR for UWB Applications

Bilal Muhammed

P.G. Scholar, Applied Electronics and Instrumentation, Lourdes Matha College of Science and Technology Thiruvananthapuram, India
bilalmuhammeds008@gmail.com

Jinju Joy

Assistant Professor, Electronics and Communication, Lourdes Matha College of Science and Technology Thiruvananthapuram, India
Jinjujoy1@gmail.com

Abstract— **In this paper, a CSRR (Complementary Split Ring Resonator) based antenna is proposed for Ultra-Wide Band Applications. The modelled structure consists of a monopole antenna loaded with CSRR and partial rectangular ground plane on the opposite side, which is fed by 50Ω microstrip transmission line. CSRR modifies the direction of current and achieve Ultra-wide band characteristics. The proposed antenna with a compact size of 28 × 23 × 1.6 mm 3 is fabricated on a FR-4 substrate of thickness of 1.6 mm, with relative dielectric constant ε_r = 4.4 and loss tangent tan δ =0. 002.The antenna had given an extra band with the introduction of CSRR.UWB behavior with better return loss characteristics are achieved by the use of CSRR. With CSRR the proposed antenna has increased its gain from 2.23 dBi to 3.58 dBi. The proposed antenna works on UWB range and can be used for Wi-Max (3.4-3.69 GHz) and WLAN (5.15-5.825 GHz) applications.**

Keywords— **Microstrip Patch Antenna, Ultra-wide band antennas, Return loss, SRR, CSRR.**

1. INTRODUCTION

The demand for compact hand held communique devices has grown considerably. Devices having inner antennas have regarded to fill this need. wireless communication structures require small length and compact antennas that have wider bandwidth than traditional antenna design [1]. Antenna length is a first-rate issue that limits device miniaturization. For the beyond few years, new designs based on the Microstrip patch antennas (MSPA) are getting used for hand-held wifi gadgets because those antennas have low-profile geometry and can be embedded into the gadgets. New wifi applications requiring operation in a couple of frequency band are rising. Twin-band and tri-band phones have received recognition due to a couple of frequency bands used for wifi applications.

Meta material-inspired antennas have concentrated on the special impact of electromagnetic wave belongings. split Ring Resonator (SRR), Complementary split Ring Resonator (CSRR) and electric powered-LC (ELC) are the primary unit factors of meta material for boosting the antenna performances. Planar monopole antenna loaded with SRR shape may be used to obtain bandwidth improvement [13] and miniaturization [14]. CSRR-loaded substrate has spurred for

appropriate impedance matching [15], multiband [16], and benefit improvement [17].

Here in this paper, a monopole antenna loaded with CSRR meta material element is supplied. UWB behavior with higher go back loss characteristics are executed by using the usage of CSRR. The antenna is proposed to operate over a bandwidth of 10.01 GHz for UWB programs. The proposed antenna works within the UWB range (4.24–14.25 GHz). This structure also can be used for C-band (4-8 GHz) applications in satellite communication, WiMAX, WiFi, C band, X band and additionally for scientific uses to discover cancers and tumors in which the safe frequency variety for human tissues is 4 GHz - 9.5 GHz.

2. ANTENNA DESIGN

The model of Microstrip Antenna can be represented by two slots of width (W) and height (h) separated by transmission line of length (L). The width of the patch can be calculated from the following equation [7].

$$W=C2fo\sqrt{2\varepsilon r+1}$$

The effective dielectric constant of the substrate can be calculated as ,

$$\varepsilon reff=\varepsilon r+12+\varepsilon r-12[1+12hW]-1/2$$

The actual length of the antenna is different from the calculated L since the fringing field also needs to be considered here. The actual length is calculated by subtracting the excess lengths from both the sides of the patch. The length of the Patch Antenna L is given by,

$$\Delta Lh=0.412(\varepsilon reff+0.3)(Wh+0.264)(\varepsilon reff-0.258)(Wh+0.8$$

Higher values of permittivity allow a shrinking of the Patch Antenna. Particularly in cell phones, the designers are given very little space and want the antenna to be a half-wavelength long. One technique is to use a substrate with a very high permittivity. The actual length of the Patch Antenna is given by,

$$Leff=C2fo\sqrt{\varepsilon reff}-2\Delta L$$

The length (Ls) and the width (Ws) of a ground plane are calculated using the following equations,

$$Lg=6h+L(3.15)$$

$$Wg=6h+W$$

Hence, if the permittivity is increased by a factor of 4, the length required decreases by a factor of 2. Using higher values for permittivity is frequently exploited in antenna miniaturization. All of the parameters in a Rectangular Patch Antenna design (L, W, h, permittivity) control the properties of the antenna. Table 1 gives the design specifications of a standard rectangular patch with FR4 substrate.

Table -1: Sample Table format

Substrate materials used	FR4(εr= 4.4)
Thickness between ground and fed patch (h)	1.6 mm
Radius of the first semicircular patch (R 1)	9.5 mm
Radius of the second semicircular patch (R 2)	4.5 mm
Width of the ground plane (Wg)	28 mm
The length of the ground plane (Lg)	23 m .

[20]

3. PARAMETRIC STUDY OF PROPOSED PATCH ANTENNA

The basic structure is that of a Proposed Patch Antenna shown in Figure.1.

The basic structure is that of a Proposed Patch Antenna shown in Figure.1.

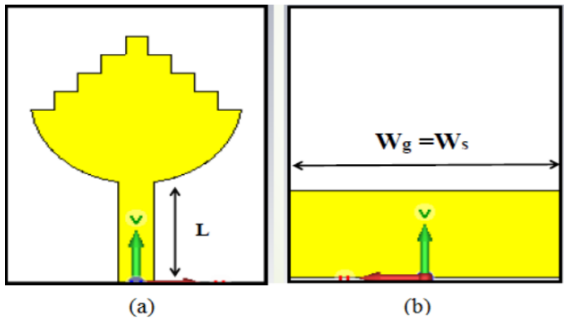

Fig -1: Proposed Patch Antenna (a) Front Side (b) Back Side

3.1 Return Loss

The response S11 shows in Figure. 2 and the antenna resonate at single frequency band, with a Return Loss maximum of -15.54 dB at resonant frequency 3.54 GHz.

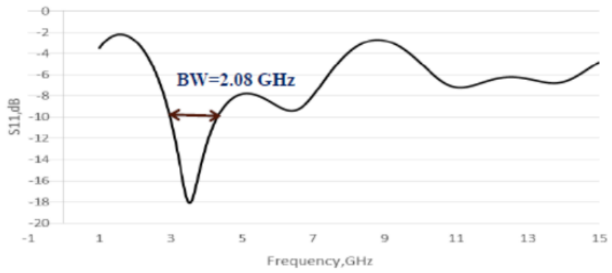

Fig -2: Plot of S11 Parameters versus Frequency of Proposed Patch

3.2 Radiation Pattern

The Radiation property of an antenna can be analyzed to understand the distribution of power around the orientation. The simulated gain pattern of the antenna can be observed at different resonant frequencies. The simulated gain pattern of the antenna shows (Figure.3) that the antenna has a gain of 2.78 dBi at first resonant frequency 3.54 GHz.

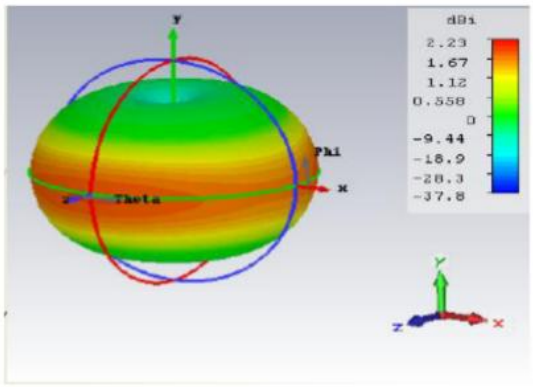

Fig -3: Radiation Pattern at 3.54 GHz

4. PARAMETRIC STUDY OF PROPOSED ANTENNA LOADED WITH CSRR

A Complementary Split Ring Resonator (CSRR) is loaded to the proposed microstrip patch antenna as shown in Figure. 4. Here two-ring split ring resonator is loaded in microstrip patch antenna substrate. Same way three-ring split ring resonator and four-ring split ring resonator are also added in the microstrip patch antenna.

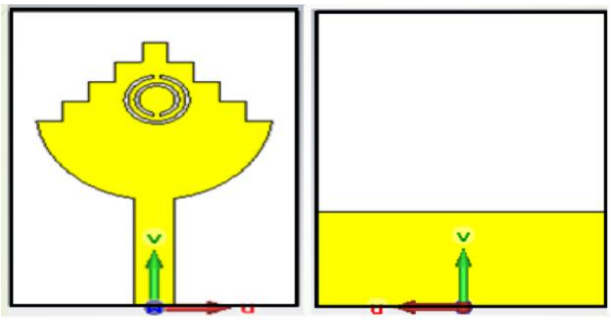

Fig -4: Proposed Patch Antenna loaded with CSRR (a) Front Side (b) Back Side

Unit Cell analysis of CSRR is shown in Fig.5. From the frequency verses permeability graph, an extra band is provided by the CSRR structure, as it shows negative resistance behavior at frequency 5.76 GHz

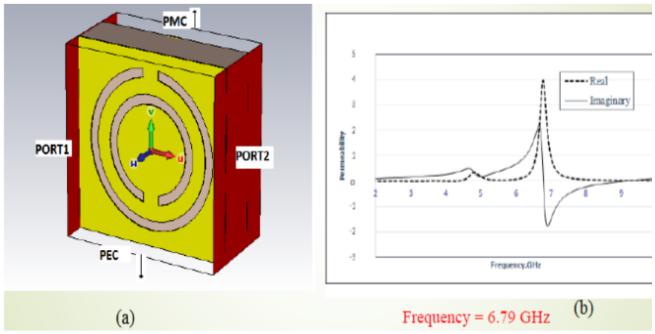

Fig -5: Unit Cell Analysis of CSRR a) Unit Cell b) Frequency Permeability Characteristics

4.1 Return Loss

The response S11 shows in Figure.6 and the antenna resonate at UWB bands, (4.24 – 14.25 GHz).

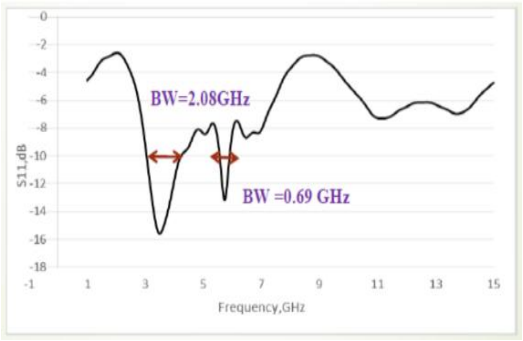

Fig -6: Plot of S11 Parameters versus Frequency of Proposed Patch loaded with CSRR

4.2 Radiation Pattern

The Radiation property of any antenna can be analyzed to understand the distribution of power around the orientation. The simulated gain pattern of the antenna shows (figure.7) that the same antenna has a gain of 3.58 dBi at second resonant frequency 5.76 GHz.

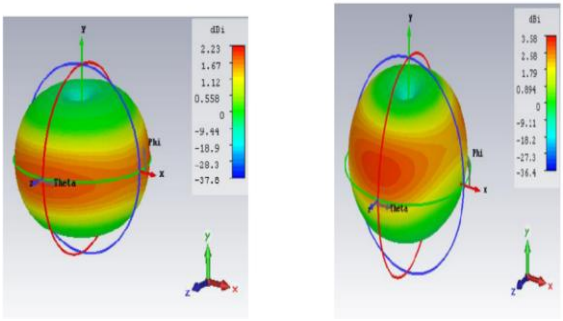

Fig -7: Radiation Patterns at 3.54 GHz (left) and Radiation Patterns at 5.76 GHz(right)

8. COMPARATIVE STUDY

Table 2 shows the comparison of proposed patch antenna loaded with and without CSRR on FR4-epoxy substrate material with dielectric constant in terms of operating frequency Band width and gain.

Table -2: Comparison with Proposed antenna loaded with and without CSRR.

Structure	Resonating Frequency (GHz)	Bandwidth (GHz)	Gain (dBi)
Proposed Patch Antenna	3.54	2.08	2.78
Proposed Antenna Loaded with CSRR	3.54	2.08	2.78
	5.76	0.69	3.58

Figure.8 shows that the simulation results of proposed antenna with and without CSRR. The simulation results give dual frequency bands bandwidth at 3.54 GHz and 5.76 GHz, which is suitable for UWB applications.

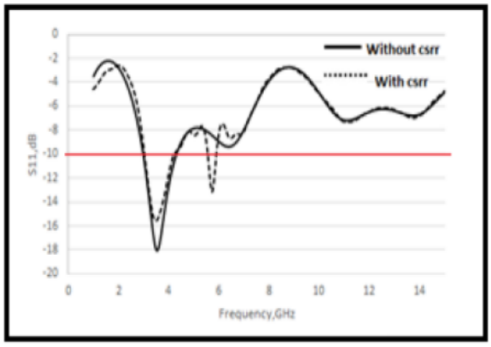

Fig -8: Comparative study of S11 Parameters versus Frequency of Proposed Patch loaded with and without CSRR.

6. CONCLUSION

The proposed antenna is evolved on 28 × 23× 1.6 mm 3 FR-4 Substrate. The CSRR within the monopole antenna creates wide-band characteristics for UWB, WiMAX and WLAN packages. The designed antenna includes a monopole antenna loaded with CSRR and partial rectangular ground plane on the alternative side. CSRR metamaterial modifies the current direction and yields ultra-wide band traits.

REFERENCES

[1] CR. Yogamathi, S. Banu, A. Vishwapriya, "Design of fractal antenna for multiband applications", IEEE-31661, ICCCNT, 4-6 July, 2013.

[2]C.Y. Liu, 2011, "An Improved Rectenna for wireless Power Transmission for Unmanned air vehicles", naval postgraduate School, Monterey, California.

[3] Chung K, Kim J, Choi J. Wideband microstrip-FED monopole antenna having frequency band-notch function. IEEE Microwave Wirel. Compon.Lett. 2005;15:766–768.[4] Vuong TP, Ghiotto A, Duroc Y, Tedjini S. Design and characteristics of a small U-slotted planar antenna for R-UWB. Microwave Opt. Technol. Lett. 2007;49:1727–1731.

[5] Abbosh AM, Bialkowoski ME, Mazierska J, Jacob MV. A planar UWB antenna with signal rejection capability in the 4–6 Hz band. IEEE MicrowaveWirel. Compon. Lett. 2006;16:278–280.

[6] Kim Y, Kwon DH. CPW-fed planar ultra wideband antenna having a frequency band notch function. Electronics Lett. 004;40:403–405.

[7] Lorena I. Basilio. 2001. The Dependence of the Input Impedance on Feed Position of Probe and Microstrip Line-Fed patch Antennas. IEEE Transaction on Antennas and Propagation. 49(1)

[8] Jayarenjini N, Ali Fathima N A, Megha S and Unni C, "Dual polarized Microstrip Fractal patch antenna for S-band Applications", IEEE Conference Publications in Control, Communication and Computing, 2015. Digital Object Identifier: 10.1109/ICCC.2015.7432941.

Bilal Muhammed procured his Mtech degree in Applied Electronics and Instrumentation from Lourdes Matha College of Science and Technology, Trivandrum, Kerala,India. He is currently working as Optical Fiber Engineer in JNET technologies private limited. Antenna designing and Analysis in CST studio is his research interest.

JINJU JOY Procured Her M Tech Degree In VLSI And Embedded Systems From Cochin University Of Science And Technology, Cochin, In 2013 And Doing Phd-Part Time. She is currently working as Assistant Professor in the Department of Electronics and Communication Engineering, Lourdes Matha College of Science and Technology, Trivandrum, Kerala, India. Her innovate scientific analysis was published by IEEE in 2013. Statistical signal processing, estimation and image fusion are her research interests